Proportional-Integral Observer Design for Multi-rate Systems Under Decode-and-Forward Relays: Tackling Power-Dependent Packet Dropouts

Di Zhao, Zidong Wang, *Fellow, IEEE*, Derui Ding, *Senior Member, IEEE*, Qing-Long Han, *Fellow, IEEE*, and Guoliang Wei

***Abstract*—In this paper, the problem of proportional-integral observer (PIO) design is investigated for a class of discrete-time multi-rate systems with multiple sensors, with the sensor sampling periods being allowed to differ from the system updating periods. The facilitation of communication between sensors and the remote PIO through wireless networks, which are subject to probabilistic packet dropouts, is achieved through the utilization of a decode-and-forward relay-based strategy. The occurrence of packet dropouts is governed by a Bernoulli-distributed random variable whose probability is dependent on the available transmission power. A decode-and-forward relay-based strategy, developed based on different components, is capable of processing information from different encoders at different physical locations. For the convenience of observer design, the lifting technique is employed with aim to cast the multi-rate system into a single-rate one. By establishing sufficient conditions, the combined effect of external noises and relaying-aided communication on estimation performance is intuitively illustrated. Subsequently, a PIO with an adjustable parameter is designed by solving certain optimization problems. A simulation example is finally provided to validate the theoretical results.**

***Index Terms*—Networked systems, proportional-integral observer design, decode-and-forward relay, power-dependent packet dropouts, multi-rate systems.**

Abbreviations and Notations

PIO	Proportional-integral observer
DaF	Decode-and-forward
StR	Sensor-to-relay
RtO	Relay-to-observer
EUBMS	Exponentially ultimately bounded in mean-square sense
AUB	Asymptotic upper bound
$\|x\|$	The Euclidean norm of x
$\mathbf{0}$	The zero matrix
$\mathbf{I}$	The identity matrix
$\lambda_{\max}(\mathscr{A})$	The maximum eigenvalue of a symmetric matrix $\mathscr{A}$
$\lambda_{\min}(\mathscr{A})$	The minimum eigenvalue of a symmetric matrix $\mathscr{A}$.

This work was supported in part by the National Natural Science Foundation of China under Grant 62273239, the Royal Society of the UK, and the Alexander von Humboldt Foundation of Germany. (*Corresponding author: Zidong Wang.*)

Di Zhao and Guoliang Wei are with the Business School, University of Shanghai for Science and Technology, Shanghai 200093, China. (Emails: zhaodi@usst.edu.cn; guoliang.wei@usst.edu.cn)

Zidong Wang is with the College of Electrical Engineering and Automation, Shandong University of Science and Technology, Qingdao 266590, China, and is also with the Department of Computer Science, Brunel University London, Uxbridge, Middlesex, UB8 3PH, United Kingdom. (Email: Zidong.Wang@brunel.ac.uk)

Derui Ding is with the Department of Control Science and Engineering, University of Shanghai for Science and Technology, Shanghai 200093, China. (Email: deruiding2010@usst.edu.cn)

Qing-Long Han is with the School of Science, Computing and Engineering Technologies, Swinburne University of Technology, Melbourne, VIC 3122, Australia. (Email: qhan@swin.edu.au)

I. Introduction

The PIO, endowed with both proportional and integral actions, offers greater design flexibility than the proportion-type observer such as the Luenberger observer. This multi-loop architecture enables the PIO to simultaneously leverage current and historical data, leading to enhanced estimation accuracy and reliability. In recent years, the PIO has attracted significant attention from the research community for its exceptional capability to manage uncertainties, delays, and imperfect data across a range of linear/nonlinear systems [3], [39], [41], [48]. Notably, the PIO has been tailored to address the challenges posed by imperfect or unreliable information in diverse contexts including artificial neural networks [4], Takagi-Sugeno fuzzy systems [45], and sensor networks [38].

It is worth noting that a prevailing assumption in the literature concerning PIO-based state estimation is the alignment of sensor sampling periods with system update intervals. Nonetheless, this assumption often falls short of practical applicability, especially in scenarios like wireless communication constrained by limited network capacities, where sensors are allowed to sample and transmit data at irregular intervals [30], [37]. This approach, known as a *multi-rate* sampling scheme, is designed to optimize network resource utilization at the cost of a marginal degradation in performance [8], [11], [12]. The adoption of multi-rate sampling, unfortunately, introduces complexities in data transmission and analytical procedures. Consequently, a considerable volume of research has been dedicated to addressing the challenges posed by multi-rate sampling [1], [19], [24], with the lifting technique being widely applied in multi-rate systems for the development of estimation algorithms [34].

Wireless communication, a pivotal technique in networked interactions, has been recently extensively adopted across diverse fields including but not limited to smart home systems, traffic management automation, and geological surveys. The advantages of this communication method are manifold, which encompass ease of system maintenance, enhanced operational flexibility, and cost-effectiveness [2], [31], [36], [46], [47].

Note that the performance of wireless communication is significantly influenced by the allocation of communication resources and the distances over which communication occurs. Constraints on communication resources can precipitate congestion in data transmission or even result in data losses, whereas communication over extensive distances may compromise data integrity [9], [10], [27], [28], [42]. Addressing these challenges is contingent upon the development and implementation of robust communication protocols, which are essential for optimizing the use of resources and maintaining the quality of communication [14], [18], [20], [21], [35], [43], [44].

Packet dropout, a widespread issue inherent to network communications, has garnered increasing attention in the realm of state estimation research [6], [7], [40]. Within the extensive literature that explores the implications of packet dropouts on data integrity, it is often posited that the probability of such dropouts remains a constant. Yet, in practical applications, this probability is subject to variation, influenced by a multitude of factors, among which transmission power stands out as a pivotal determinant. It is intuitive to anticipate that an increase in transmission power correlates with a decrease in the likelihood of packet dropouts. Nonetheless, the application of higher transmission power is frequently curtailed by the limitations of available resources, thereby complicating the assurance of dependable data transmission within wireless digital networks. Consequently, tackling the ramifications of transmission power limitations on the state estimation process is imperative for the sustenance of efficacious data communication.

To enhance communication quality across extended distances, a straightforward approach involves segmenting the lengthy wireless route into shorter spans, thereby facilitating relay-assisted communication. In such relay-based communication frameworks, relays are tasked with receiving signals, processing the data, and subsequently forwarding these signals to distant endpoints [5], [23]. In engineering realms, a variety of relay strategies find application, notable among them are amplify-and-forward relays [15], [16], compress-and-forward relays [13], compute-and-forward relays [26], filter-and-forward relays [29], and DaF relays [17]. Specifically, DaF relays engage in the encoding and decoding of received signals prior to their transmission to the intended destinations. Recent years have seen emerging research interest in networked systems that integrate DaF relays [22], [25]. Presently, the challenge of formulating a PIO design that incorporates DaF relay-based strategies, particularly in contexts where packet dropout is influenced by transmission power, stands as an unexplored research frontier, and overcoming this challenge constitutes a key objective of our current research efforts.

Driven by the preceding deliberations, this paper addresses the problem of designing PIOs for multi-rate systems affected by power-dependent packet dropouts, utilizing component-based DaF relays. The core difficulties encountered in this domain encompass: 1) formulating a viable strategy to mitigate the transmission challenges arising from the inherently unreliable wireless network communication; 2) delineating the cumulative impact of transmission power, ambient noise, and relay-supported communication on the efficacy of state estimation; and 3) identifying the optimal gains for the PIO that take into account the multifaceted nature of the factors involved.

In response to the challenges identified earlier, this paper makes the following significant contributions.

1) This paper represents an inaugural effort to the exploration of the PIO design problem within the context of DaF relayed communication.
2) A novel component-based DaF relay strategy is introduced, which not only markedly enhances the quality of communication over extended distances, but also facilitates the decoder's ability to assimilate information from various encoders dispersed across different locales.
3) An investigation is conducted into the collective influence of power-dependent packet dropout, external noise, and relay-assisted communication on the design of PIOs for multi-rate systems.
4) The development of a PIO endowed with a tunable parameter is achieved, which ensures the estimation error dynamics to be EUBMS. This development represents a substantial leap forward in enhancing PIO performance, striking an optimal balance between estimation precision and rate of convergence.

The organization of this paper is structured as follows. Section II delivers an extensive exposition of the constituent elements, encompassing the system model, the model of transmission, the architecture of the PIO, and the index of performance. Section III elucidates the principal results pertaining to boundedness analysis and delineates the approach for the determination of observer gains. Section IV is dedicated to the exhibition of simulation outcomes that corroborate the efficacy of the methodology proposed. Section V draws the paper to a close by encapsulating the primary insights and contributions yielded by the study.

II. Problem Formulation and Preliminaries

A. System Model

Consider a class of linear discrete-time systems of the following form:

$$x(z_{p+1}) = Ax(z_p) + Bw(z_p) \tag{1}$$

where $x(z_p) \in \mathbb{R}^{n_x}$ is the system state and $w(z_p) \in \mathbb{W} \triangleq \{w : \|w\|^2 \leqslant \bar{w};\ w \in \mathbb{R}^{n_w}\}$ is the exogenous disturbance with $\bar{w} > 0$ being a known scalar. A and B are known matrices with appropriate dimensions. Here, z_p $(p = 0, 1, 2, \ldots)$ is the state updating instant of system (1), and $z_{p+1} - z_p = \jmath$ is the state updating period with $\jmath$ being a known positive integer.

The system described by (1) is considered to be monitored by n sensors, which are distributed across various physical locations. The measurement obtained from sensor i is modeled by

$$y^{[i]}(d_p) = C^{[i]}x(d_p) \tag{2}$$

for $i \in \mathfrak{I} \triangleq \{1, 2, \ldots, n\}$, where $y^{[i]}(d_p) \in \mathbb{R}$ is the measurement value of sensor i, $C^{[i]}$ is known matrix with compatible dimension, and d_p $(p = 0, 1, 2, \ldots)$ is the sampling instant of sensors satisfying $d_{p+1} - d_p = h\jmath$ with h being a known

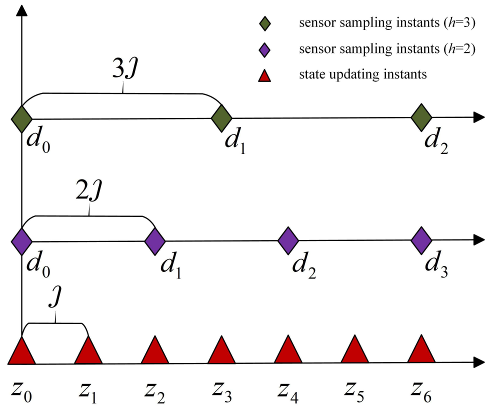

Fig. 1: The illustration of multi-rate sampling mechanism.

positive integer. Assume that $z_0 = d_0 = 0$. Fig. 1 depicts the rules for state updating and sensor sampling with different integer h.

B. Communication Network

To alleviate the challenges posed by the unreliable nature of wireless network communication, especially in the context of long-distance transmissions, a DaF relay-based protocol is utilized during the data transmission process from sensors to the remote state observer. In practical scenarios, data transmission from sensors, which are distributed across various locations, may encounter diverse communication environments. These environments can differ in several aspects, such as transmission distances, data resolution requirements, and transmission power levels. Consequently, the parameters of the DaF relay-based protocol are tailored specifically for the different components, taking into account their unique communication environments.

As depicted in Fig. 2, the transmission of measurement outputs to the observer comprises two distinct phases: the StR transmission and the RtO transmission. During the StR phase, the measurement outputs are initially encoded into specific binary codewords by the encoders, followed by the decoding of these codewords by the decoder. The decoded signals are then forwarded to the relay. In the subsequent RtO phase, the transmission is subject to probabilistic packet dropouts, a consequence of the inherent unreliability of wireless communication.

1) StR transmission: Prior to transmission, the measurement $y^{[i]}(d_p)$ obtained by sensor i (where i belongs to the set $\mathfrak{I}$) is converted into the index $\kappa^{[i]}(d_p)$ through the encoding function $\acute{\flat}^{[i]}(\cdot)$, which is defined as follows:

$$\kappa^{[i]}(d_p) = \acute{\flat}^{[i]}\big(y^{[i]}(d_p)\big). \tag{3}$$

Subsequently, for the index $\kappa^{[i]}(d_p)$, a codeword is generated as:

$$\acute{y}^{[i]}(d_p) = \begin{bmatrix} \acute{\kappa}^{[i]} & \kappa^{[i]}(d_p) \end{bmatrix}, \tag{4}$$

where $\acute{\kappa}^{[i]}$ serves as a reference to the sensor label.

For encoding the data, a scalar uniform quantizer $\Omega^{[i]}(.) : \mathbb{R} \to \mathbb{R}$ is utilized to generate the codeword. By choosing a scale parameter $\gamma^{[i]}$ and an integer $\delta^{[i]}$, the interval $[-\gamma^{[i]}, \gamma^{[i]}]$ is uniformly partitioned into $\delta^{[i]}$ subintervals with the qth subinterval $\mathbb{M}_q^{[i]}(\gamma^{[i]})$ $\big(q \in \mathfrak{D}^{[i]} \triangleq \{1, 2, \ldots, \delta^{[i]}\}\big)$ described as

$$\mathbb{M}_q^{[i]}(\gamma^{[i]}) = \left[-\frac{\gamma^{[i]} + (2q-1)\gamma^{[i]}}{\delta^{[i]}}, -\frac{\gamma^{[i]} + 2q\gamma^{[i]}}{\delta^{[i]}}\right)$$

and

$$\mathbb{M}_a^{[i]}(\gamma^{[i]}) \bigcap \mathbb{M}_b^{[i]}(\gamma^{[i]}) = \emptyset$$

for any $(a, b \in \mathfrak{D}^{[i]})$ and $a \neq b$. Correspondingly, the scalar uniform quantizer has the following form:

$$\Omega^{[i]}(o^{[i]}) = \begin{cases} \gamma^{[i]}, & o^{[i]} \geqslant \gamma^{[i]} \\ -\gamma^{[i]}, & o^{[i]} \leqslant -\gamma^{[i]} \\ -\gamma^{[i]} + \dfrac{(2\hbar^{[i]}-1)\gamma^{[i]}}{\delta^{[i]}}, & \acute{\gamma}^{[i]} \leqslant o^{[i]} \leqslant \grave{\gamma}^{[i]} \end{cases} \tag{5}$$

where $o^{[i]}$ denotes the signal to be processed and

$$\acute{\gamma}^{[i]} \triangleq -\gamma^{[i]} + \frac{2(\hbar^{[i]}-1)\gamma^{[i]}}{\delta^{[i]}}$$
$$\grave{\gamma}^{[i]} \triangleq -\gamma^{[i]} + \frac{2\hbar^{[i]}\gamma^{[i]}}{\delta^{[i]}}, \quad \hbar^{[i]} \in \mathfrak{D}^{[i]}.$$

To prevent quantizer saturation, an adaptive parameter $\theta^{[i]}$ is incorporated into the quantization process as follows:

$$\Omega^{[i]}\big(y^{[i]}(d_p)\big) \triangleq \theta^{[i]}\Omega^{[i]}\left(\frac{y^{[i]}(d_p)}{\theta^{[i]}}\right), \tag{6}$$

ensuring that when $\big|y^{[i]}(d_p)\big| > \gamma^{[i]}$, the ratio $y^{[i]}(d_p)/\theta^{[i]}$ falls within the interval $\big[-\gamma^{[i]}, \gamma^{[i]}\big]$.

Denoting $\zeta^{[i]}(d_p) \triangleq \Omega^{[i]}\big(y^{[i]}(d_p)\big) - y^{[i]}(d_p)$ as the component quantization error, it is easy to derive that

$$\Big|\zeta^{[i]}(d_p)\Big| \leqslant \frac{\theta^{[i]}\gamma^{[i]}}{\delta^{[i]}}. \tag{7}$$

For any $\Omega^{[i]}\big(y^{[i]}(d_p)\big) \in \mathbb{M}_q^{[i]}(\gamma^{[i]})$, there exists an integer $\kappa^{[i]}(d_p)$ such that

$$\acute{\flat}^{[i]}\Big(\Omega^{[i]}\big(y^{[i]}(d_p)\big)\Big) = \kappa^{[i]}(d_p). \tag{8}$$

For any codeword $\acute{y}^{[i]}(d_p)$, the sensor label $\ell^{[i]}$ is extracted by:

$$\ell^{[i]} = \acute{y}^{[i]}(d_p)\begin{bmatrix} 1 \\ 0 \end{bmatrix}. \tag{9}$$

Correspondingly, the decoded signal is obtained by the decoding function $\grave{\flat}^{[i]}(\cdot)$ of the following form:

$$\grave{y}^{[i]}(d_p) = \grave{\flat}^{[i]}\big(\kappa^{[i]}(d_p)\big) = -\gamma^{[i]} + \frac{(2\kappa^{[i]}(d_p)-1)\gamma^{[i]}}{\delta^{[i]}} \tag{10}$$

where $\grave{y}^{[i]}(d_p)$ is the decoded value of $y^{[i]}(d_p)$.

Letting $\xi^{[i]}(d_p) \triangleq \grave{\flat}^{[i]}\big(\kappa^{[i]}(d_p)\big) - y^{[i]}(d_p)$ be the decoding error, it is not difficult to obtain

$$\xi^{[i]}(d_p) = \zeta^{[i]}(d_p) \leqslant \frac{\theta^{[i]}\gamma^{[i]}}{\delta^{[i]}}. \tag{11}$$

Accordingly, the output of the decoder can be expressed by

$$\grave{y}^{[i]}(d_p) = y^{[i]}(d_p) + \xi^{[i]}(d_p). \tag{12}$$

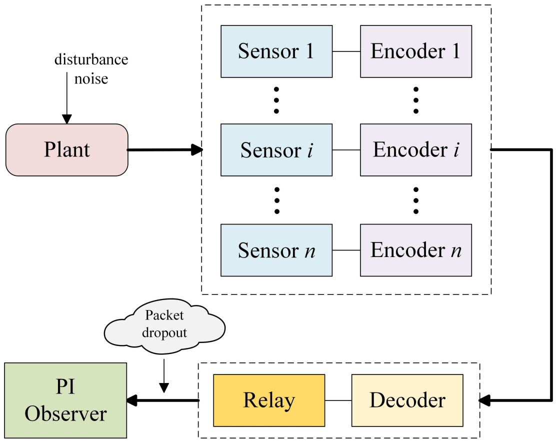

Fig. 2: PIO design under DaF relay.

Defining

$$\begin{aligned}\grave{y}(d_p) &\triangleq \operatorname{col}\left\{\grave{y}^{[1]}(d_p),\ \grave{y}^{[2]}(d_p),\ \ldots,\ \grave{y}^{[n]}(d_p)\right\}\\ \xi(d_p) &\triangleq \operatorname{col}\left\{\xi^{[1]}(d_p),\ \xi^{[2]}(d_p),\ \ldots,\ \xi^{[n]}(d_p)\right\},\end{aligned}$$

one further obtains

$$\grave{y}(d_p) = y(d_p) + \xi(d_p). \tag{13}$$

2) RtO transmission: The transmission of the signal from the relay to the observer is influenced by probabilistic packet dropout, resulting in the following actually received signal:

$$\breve{y}(d_p) = \iota(d_p)\sqrt{\epsilon}\grave{y}(d_p) + Gv(d_p), \tag{14}$$

where $\breve{y}(d_p)$ denotes the relayed signal received by the observer, ϵ represents the available transmission power, and G is a known matrix with suitable dimensions. The term $v(d_p)$ stands for the channel noise satisfying $\|v(d_p)\|^2 \leqslant \bar{v}$. The Bernoulli random variable $\iota(d_p)$ is introduced to govern the probabilistic packet dropout in the following manner:

$$\operatorname{Prob}\{\iota(d_p)\} = \begin{cases} 0, & \text{packet dropout occurs} \\ 1, & \text{no packet dropout occurs.}\end{cases} \tag{15}$$

Correspondingly, the probability distribution of $\iota(d_p)$ is characterized by:

$$\operatorname{Prob}\{\iota(d_p) = 0\} = \bar{\iota}(\epsilon),\ \operatorname{Prob}\{\iota(d_p) = 1\} = 1 - \bar{\iota}(\epsilon) \tag{16}$$

where $\bar{\iota}(\epsilon) \triangleq \exp(-\mu\epsilon)$ with $\mu > 0$ being a known scalar related to the channel's statistical properties.

Remark 1: The technology of relaying-aid communication stands as a potent solution for enhancing long-distance wireless communication, primarily by subdividing the extensive wireless path into shorter segments. In alignment with this principle, our study adopts a DaF relay-based strategy by segmenting the signal transmission from sensors to the remote PIO into two distinct phases: the StR transmission and the RtO transmission. As delineated in (14), the measurement actually received by the observer is intricately linked to several factors including the decoding error, channel noises, transmission power, and the probabilistic nature of packet dropouts. This interrelation introduces a significant challenge since it can potentially complicate the dynamics of signal transmission as well as the processes involved in analysis and synthesis.

Remark 2: The stochastic nature of packet dropouts is modeled using a Bernoulli-distributed sequence, where the dropout probability is dependent on the available transmission power ϵ. This modeling approach is widely adopted in communication studies, particularly for scenarios involving Rayleigh channel fading [32], [33]. In this context, $\iota(d_p) = 0$ signifies a "failed" transmission, resulting in data loss, whereas $\iota(d_p) = 1$ denotes a "successful" transmission, with the data successfully reaching the remote observer. Importantly, as indicated by (16), an increase in transmission power ϵ is associated with a decrease in the probability of packet dropout $\bar{\iota}(\epsilon)$, illustrating the impact of transmission power on communication reliability.

C. The PIO

Considering both (1) and (14), and introducing the following notations:

$$\begin{aligned}
\bar{x}(d_p) &\triangleq \operatorname{col}\{x(d_{p-1} + \jmath),\ x(d_{p-1} + 2\jmath),\ \ldots,\ x(d_p)\}\\
\bar{w}(d_p) &\triangleq \operatorname{col}\{w(d_p),\ w(d_p + \jmath),\ \ldots,\ w(d_p + (h-1)\jmath)\}\\
\bar{A} &\triangleq \begin{bmatrix} \underbrace{\mathbf{0}_{hn_x\times n_x} \ \cdots \ \mathbf{0}_{hn_x\times n_x}}_{h-1} & \bar{A}_0 \end{bmatrix}\\
\bar{B} &\triangleq \begin{bmatrix} B & \mathbf{0} & \mathbf{0} & \cdots & \mathbf{0} \\ AB & B & \mathbf{0} & \cdots & \mathbf{0} \\ A^2B & AB & B & \cdots & \mathbf{0} \\ \vdots & \vdots & \vdots & \ddots & \vdots \\ A^{h-1}B & A^{h-2}B & A^{h-3}B & \cdots & B \end{bmatrix}\\
\bar{A}_0 &\triangleq \operatorname{col}\left\{A,\ A^2,\ \ldots,\ A^h\right\}\\
C &\triangleq \operatorname{col}\left\{C^{[1]},\ C^{[2]},\ \ldots,\ C^{[n]}\right\}\\
\bar{C} &\triangleq \begin{bmatrix} \underbrace{\mathbf{0}_{n\times n_x} \ \cdots \ \mathbf{0}_{n\times n_x}}_{h-1} & C \end{bmatrix},
\end{aligned}$$

we obtain the following single-rate system:

$$\begin{cases} \bar{x}(d_{p+1}) = \bar{A}\bar{x}(d_p) + \bar{B}\bar{w}(d_p) \\ \breve{y}(d_p) = \iota(d_p)\sqrt{\epsilon}\bar{C}\bar{x}(d_p) + Gv(d_p) \\ \qquad\quad + \iota(d_p)\sqrt{\epsilon}\xi(d_p) \end{cases}. \tag{17}$$

In this paper, to estimate the states of (17), the following PIO is adopted:

$$\begin{cases} \hat{x}(d_{p+1}) = \bar{A}\hat{x}(d_p) + H_1 s(d_p) \\ \qquad\qquad + H_2\big(\breve{y}(d_p) - \hat{y}(d_p)\big) \\ s(d_{p+1}) = s(d_p) + H_3\big(\breve{y}(d_p) - \hat{y}(d_p)\big) \end{cases} \tag{18}$$

where $\hat{y}(d_p) \triangleq \bar{C}\hat{x}(d_p)$; $\hat{x}(d_p)$ is the estimate of $\bar{x}(d_p)$; $s(d_p)$ is the integral of the output estimation error; H_1, H_2 and H_3 are observer gains to be designed.

By defining the state estimation error and the augmented state vector, respectively, as follows:

$$\tilde{x}(d_p) \triangleq \bar{x}(d_p) - \hat{x}(d_p),\ \Im(d_p) \triangleq \operatorname{col}\{\tilde{x}(d_p),\ s(d_p),\ \bar{x}(d_p)\},$$

we derive from (17)–(18) that

$$\begin{aligned}\Im(d_{p+1}) =& \mathcal{A}_1\Im(d_p) + \aleph(d_p)\mathcal{A}_2\Im(d_p) \\ &+ \mathcal{M}_1\xi(d_p) + \aleph(d_p)\mathcal{M}_2\xi(d_p) \\ &+ \mathcal{B}_1\bar{w}(d_p) + \mathcal{B}_2 v(d_p)\end{aligned} \tag{19}$$

where

$$\mathcal{A}_1 \triangleq \begin{bmatrix} \bar{A} - H_2\bar{C} & -H_1 & -H_2\bar{C} - \bar{\iota}(\epsilon)\sqrt{\epsilon}H_2\bar{C} \\ H_3\bar{C} & \mathbf{I} & \bar{\iota}(\epsilon)\sqrt{\epsilon}H_3\bar{C} - H_3\bar{C} \\ \mathbf{0} & \mathbf{0} & \bar{A} \end{bmatrix}$$

$$\mathcal{A}_2 \triangleq \begin{bmatrix} \mathbf{0} & \mathbf{0} & -\sqrt{\epsilon}H_2\bar{C} \\ \mathbf{0} & \mathbf{0} & \sqrt{\epsilon}H_3\bar{C} \\ \mathbf{0} & \mathbf{0} & \mathbf{0} \end{bmatrix}, \quad \mathcal{B}_1 \triangleq \begin{bmatrix} \bar{B} \\ \mathbf{0} \\ \bar{B} \end{bmatrix}$$

$$\mathcal{B}_2 \triangleq \begin{bmatrix} -H_2G \\ H_3G \\ \mathbf{0} \end{bmatrix}, \quad \aleph(d_p) \triangleq \iota(d_p) - 1 + \bar{\iota}(\epsilon)$$

$$\mathcal{M}_1 \triangleq \begin{bmatrix} -\bar{\iota}(\epsilon)\sqrt{\epsilon}H_2 \\ \bar{\iota}(\epsilon)\sqrt{\epsilon}H_3 \\ \mathbf{0} \end{bmatrix}, \quad \mathcal{M}_2 \triangleq \begin{bmatrix} -\sqrt{\epsilon}H_2 \\ \sqrt{\epsilon}H_3 \\ \mathbf{0} \end{bmatrix}.$$

D. Main Objective

Definition 1: The augmented system (19) is said to be EUBMS if there are scalars $0 < \alpha_1 < 1$, $\alpha_2 > 0$ and $\alpha_3 > 0$ such that

$$\mathbb{E}\{\|\Im(d_p)\|^2\} \leqslant \alpha_1^{d_p}\alpha_2 + \alpha_3, \quad \forall d_p \geqslant 0 \tag{20}$$

where α_3 is called the AUB of $\|\Im(d_p)\|^2$ in mean-square sense.

The objective of this paper is to obtain conditions that ensure system (19) to be EUBMS and then determine the PIO gains H_1, H_2 and H_3 to minimize the AUB while maximizing the decay rate.

III. Main Results

A. Design of Encoding and Decoding Procedures

As discussed in the previous section, the encoding procedure and the decoding procedure are essential in DaF relay-based data transmission. In this subsection, we are interested in formalizing the encoding procedure and the decoding procedure.

According to (3)–(9), the detailed encoding process can be summarized in Algorithm 1.

Algorithm 1 Component-Based Encoding Procedure

Step 1. Let the measurement $y^{[i]}(d_p)$, the scale parameter $\gamma^{[i]}$, and the quantization level $\delta^{[i]}$ be given.
Step 2. According to the sensor label, figure out $\acute{\kappa}^{[i]}$ as the first component of the codeword $\acute{y}^{[i]}(d_p)$.
Step 3. Find a $\theta^{[i]}$, such that $\frac{y^{[i]}(d_p)}{\theta^{[i]}} \in \left[-\gamma^{[i]},\, \gamma^{[i]}\right]$.
Step 4. According to (5)–(6), figure out integer q such that $\Omega^{[i]}\big(y^{[i]}(d_p)\big) \in \mathbb{M}_q^{[i]}(\gamma^{[i]})$.
Step 5. According to (8), figure out the index $\kappa^{[i]}(d_p)$ as the second component of the codeword $\acute{y}^{[i]}(d_p)$.
Step 6. Obtain and output the codeword $\acute{y}^{[i]}(d_p)$ of the form $[\acute{\kappa}^{[i]},\, \kappa^{[i]}(d_p)]$.

Based on the discussions in (10)–(13), the detailed steps of the decoding procedure are outlined in Algorithm 2.

Algorithm 2 Decoding Procedure

Step 1. If the codeword $\acute{y}^{[i]}(d_p)$ $(i \in \mathfrak{I})$ is accessible, go to next step, else go to *Step 6*.
Step 2. According to (9), figure out the sensor label $\ell^{[i]}$.
Step 3. Looking up the corresponding alphabet, figure out the parameters $\gamma^{[i]}$ and $\delta^{[i]}$.
Step 4. According to (10), figure out the decoded measurement $\grave{y}^{[i]}(d_p)$.
Step 5. If there is another codeword $\acute{y}^{[i]}(d_p)$ $(i \in \mathfrak{I})$, go to *Step 2*, else go to *Step 6*.
Step 6. Stop.

B. Analysis of the PIO

In Theorem 1, we aim to establish the conditions which guarantee that the augmented system (19) is EUBMS.

Theorem 1: Consider the augmented system (19) with the PIO (18). Assume that parameters H_1, H_2 and H_3 are given. Then, the augmented system (19) is EUBMS if there exist positive scalars η_1, η_2, η_3, η_4, and positive definite matrix Θ such that

$$\Re^{(1)} = \begin{bmatrix} \Re^{(1)}_{(11)} & \star \\ \Re^{(1)}_{(21)} & \Re^{(1)}_{(22)} \end{bmatrix} < 0 \tag{21}$$

with

$$\begin{aligned}\Re^{(1)}_{(11)} \triangleq& \mathrm{diag}\{-\Theta + \eta_1\Theta,\ -\eta_2\mathbf{I},\ -\eta_3\mathbf{I},\ -\eta_4\mathbf{I}\} \\ \Re^{(1)}_{(21)} \triangleq& \begin{bmatrix} \hat{\aleph}\mathcal{A}_2 & \hat{\aleph}\mathcal{M}_2 & \mathbf{0} & \mathbf{0} \\ \mathcal{A}_1 & \mathcal{M}_1 & \mathcal{B}_1 & \mathcal{B}_2 \end{bmatrix} \\ \Re^{(1)}_{(21)} \triangleq& -\mathbf{I}_2 \otimes \Theta^{-1}, \quad \hat{\aleph} \triangleq \sqrt{\bar{\iota}(\epsilon) - \bar{\iota}^2(\epsilon)}.\end{aligned}$$

Correspondingly, the AUB is given by

$$\alpha_3 \triangleq \frac{1}{\lambda_{\min}(\Theta)\eta_1}\left(\eta_2\sum_{i=1}^{n}\left(\frac{\theta^{[i]}\gamma^{[i]}}{\delta^{[i]}}\right)^2 + \eta_3 h\bar{w} + \eta_4\bar{v}\right). \tag{22}$$

Proof: Choose the following Lyapunov function candidate:

$$V\big(\Im(d_p)\big) \triangleq \Im^T(d_p)\Theta\Im(d_p) \tag{23}$$

with its difference given by

$$\triangle V\big(\Im(d_p)\big) \triangleq \mathbb{E}\{V\big(\Im(d_{p+1})\big)|\Im(d_p)\} - V\big(\Im(d_p)\big). \tag{24}$$

According to (23)–(24), the mathematical expectation of $\triangle V\big(\Im(d_p)\big)$ is calculated by

$$\begin{aligned}&\mathbb{E}\{\triangle V\big(\Im(d_p)\big)\} \\ =&\mathbb{E}\big\{V\big(\Im(d_{p+1})\big) - V\big(\Im(d_p)\big)\big\} \\ =&\mathbb{E}\Big\{\Big(\mathcal{A}_1\Im(d_p) + \aleph(d_p)\mathcal{A}_2\Im(d_p) + \mathcal{M}_1\xi(d_p) \\ &+ \aleph(d_p)\mathcal{M}_2\xi(d_p) + \mathcal{B}_1\bar{w}(d_p) + \mathcal{B}_2v(d_p)\Big)^T\Theta \\ &\times\Big(\mathcal{A}_1\Im(d_p) + \aleph(d_p)\mathcal{A}_2\Im(d_p) + \mathcal{M}_1\xi(d_p) \\ &+ \aleph(d_p)\mathcal{M}_2\xi(d_p) + \mathcal{B}_1\bar{w}(d_p) + \mathcal{B}_2v(d_p)\Big) \\ &- \Im^T(d_p)\Theta\Im(d_p)\Big\} \\ =&\mathbb{E}\Big\{\Im^T(d_p)\big(\mathcal{A}_1^T\Theta\mathcal{A}_1 + \hat{\aleph}^2\mathcal{A}_2^T\Theta\mathcal{A}_2 - \Theta\big)\Im(d_p) \\ &+ \xi^T(d_p)\big(\mathcal{M}_1^T\Theta\mathcal{M}_1\xi(d_p) + \hat{\aleph}^2\mathcal{M}_2^T\Theta\mathcal{M}_2\big)\xi(d_p)\end{aligned}$$

$$
\begin{aligned}
&+\bar{w}^T(d_p)\mathcal{B}_1^T\Theta\mathcal{B}_1\bar{w}(d_p)+v^T(d_p)\mathcal{B}_2^T\Theta\mathcal{B}_2v(d_p)\\
&+2\xi^T(d_p)\mathcal{M}_1^T\Theta\mathcal{A}_1\Im(d_p)+2\bar{w}^T(d_p)\mathcal{B}_1^T\Theta\mathcal{A}_1\Im(d_p)\\
&+2v^T(d_p)\mathcal{B}_2^T\Theta\mathcal{A}_1\Im(d_p)+2\hat{\aleph}^2\xi^T(d_p)\mathcal{M}_2^T\Theta\mathcal{A}_2\Im(d_p)\\
&+2\bar{w}^T(d_p)\mathcal{B}_1^T\Theta\mathcal{M}_1\xi(d_p)+2v^T(d_p)\mathcal{B}_2^T\Theta\mathcal{M}_1\xi(d_p)\\
&+2v^T(d_p)\mathcal{B}_2^T\Theta\mathcal{B}_1\bar{w}(d_p)\Big\}\\
=&\mathbb{E}\Big\{\Im^T(d_p)\big(\mathcal{A}_1^T\Theta\mathcal{A}_1+\hat{\aleph}^2\mathcal{A}_2^T\Theta\mathcal{A}_2-\Theta+\eta_1\Theta\big)\Im(d_p)\\
&+\xi^T(d_p)\big(\mathcal{M}_1^T\Theta\mathcal{M}_1\xi(d_p)+\hat{\aleph}^2\mathcal{M}_2^T\Theta\mathcal{M}_2-\eta_2\mathbf{I}\big)\xi(d_p)\\
&+\bar{w}^T(d_p)\big(\mathcal{B}_1^T\Theta\mathcal{B}_1-\eta_3\mathbf{I}\big)\bar{w}(d_p)+v^T(d_p)\big(\mathcal{B}_2^T\Theta\mathcal{B}_2\\
&-\eta_4\mathbf{I}\big)v(d_p)+2\xi^T(d_p)\mathcal{M}_1^T\Theta\mathcal{A}_1\Im(d_p)+2\bar{w}^T(d_p)\\
&\times\mathcal{B}_1^T\Theta\mathcal{A}_1\Im(d_p)+2v^T(d_p)\mathcal{B}_2^T\Theta\mathcal{A}_1\Im(d_p)\\
&+2\hat{\aleph}^2\xi^T(d_p)\mathcal{M}_2^T\Theta\mathcal{A}_2\Im(d_p)+2\bar{w}^T(d_p)\mathcal{B}_1^T\Theta\mathcal{M}_1\xi(d_p)\\
&+2v^T(d_p)\mathcal{B}_2^T\Theta\mathcal{M}_1\xi(d_p)+2v^T(d_p)\mathcal{B}_2^T\Theta\mathcal{B}_1\bar{w}(d_p)\\
&-\eta_1V\big(\Im(d_p)\big)+\eta_2\xi^T(d_p)\xi(d_p)+\eta_3\bar{w}^T(d_p)\bar{w}(d_p)\\
&+\eta_4v^T(d_p)v(d_p)\Big\}\\
=&\mathbb{E}\big\{\chi^T(d_p)\Pi\chi(d_p)-\eta_1V\big(\Im(d_p)\big)+\eta_2\xi^T(d_p)\xi(d_p)\\
&+\eta_3\bar{w}^T(d_p)\bar{w}(d_p)+\eta_4v^T(d_p)v(d_p)\big\}
\end{aligned}\tag{25}
$$

where

$$
\begin{aligned}
\chi(d_p)\triangleq&\ \mathrm{col}\left\{\Im(d_p),\ \xi(d_p),\ \bar{w}(d_p),\ v(d_p)\right\}\\
\Pi\triangleq&\begin{bmatrix}\Pi^{(11)}&\star&\star&\star\\ \Pi^{(21)}&\Pi^{(22)}&\star&\star\\ \Pi^{(31)}&\Pi^{(32)}&\Pi^{(33)}&\star\\ \Pi^{(41)}&\Pi^{(42)}&\Pi^{(43)}&\Pi^{(44)}\end{bmatrix}\\
\Pi^{(11)}\triangleq&\mathcal{A}_1^T\Theta\mathcal{A}_1+\hat{\aleph}^2\mathcal{A}_2^T\Theta\mathcal{A}_2-\Theta+\eta_1\Theta\\
\Pi^{(22)}\triangleq&\mathcal{M}_1^T\Theta\mathcal{M}_1\xi(d_p)+\hat{\aleph}^2\mathcal{M}_2^T\Theta\mathcal{M}_2-\eta_2\mathbf{I}\\
\Pi^{(33)}\triangleq&\mathcal{B}_1^T\Theta\mathcal{B}_1-\eta_3\mathbf{I},\quad \Pi^{(44)}\triangleq\mathcal{B}_2^T\Theta\mathcal{B}_2-\eta_4\mathbf{I}\\
\Pi^{(21)}\triangleq&\mathcal{M}_1^T\Theta\mathcal{A}_1+\hat{\aleph}^2\mathcal{M}_2^T\Theta\mathcal{A}_2,\ \Pi^{(31)}\triangleq\mathcal{B}_1^T\Theta\mathcal{A}_1\\
\Pi^{(32)}\triangleq&\mathcal{B}_1^T\Theta\mathcal{M}_1,\quad \Pi^{(41)}\triangleq\mathcal{B}_2^T\Theta\mathcal{A}_1\\
\Pi^{(42)}\triangleq&\mathcal{B}_2^T\Theta\mathcal{M}_1,\quad \Pi^{(43)}\triangleq\mathcal{B}_2^T\Theta\mathcal{B}_1.
\end{aligned}
$$

Applying Schur Complement Lemma to (21) in Theorem 1, we have $\Pi<0$, which implies

$$
\begin{aligned}
&\mathbb{E}\{\triangle V\big(\Im(d_p)\big)\}\\
\leqslant&-\eta_1\mathbb{E}\big\{V\big(\Im(d_p)\big)\big\}+\eta_2\xi^T(d_p)\xi(d_p)\\
&+\eta_3\bar{w}^T(d_p)\bar{w}(d_p)+\eta_4v^T(d_p)v(d_p).
\end{aligned}\tag{26}
$$

From the definitions of $\xi(d_p)$, $\bar{w}(d_p)$ and $v(d_p)$, one derives that

$$
\begin{aligned}
\xi^T(d_p)\xi(d_p)\leqslant&\sum_{i=1}^{n}\left(\frac{\theta^{[i]}\gamma^{[i]}}{\delta^{[i]}}\right)^2\\
\bar{w}^T(d_p)\bar{w}(d_p)\leqslant&\ h\bar{w}\\
v^T(d_p)v(d_p)\leqslant&\bar{v}.
\end{aligned}\tag{27}
$$

Therefore, one has from (26) that

$$
\mathbb{E}\{\triangle V\big(\Im(d_p)\big)\}\leqslant-\eta_1\mathbb{E}\big\{V\big(\Im(d_p)\big)\big\}+\bar{\imath}\tag{28}
$$

with

$$
\bar{\imath}\triangleq\eta_2\sum_{i=1}^{n}\left(\frac{\theta^{[i]}\gamma^{[i]}}{\delta^{[i]}}\right)^2+\eta_3h\bar{w}+\eta_4\bar{v}.\tag{29}
$$

For any $\upsilon>1$, it is derived from (25) and (28) that

$$
\begin{aligned}
&\mathbb{E}\big\{\upsilon^{d_{p+1}}V\big(\Im(d_{p+1})\big)\big\}-\mathbb{E}\big\{\upsilon^{d_p}V\big(\Im(d_p)\big)\big\}\\
=&\upsilon^{d_{p+1}}\mathbb{E}\big\{\triangle V\big(\Im(d_p)\big)\big\}+\upsilon^{d_p}(\upsilon^{h_J}-1)\mathbb{E}\big\{V\big(\Im(d_p)\big)\big\}\\
\leqslant&\upsilon^{d_{p+1}}\Big(-\eta_1\mathbb{E}\big\{V\big(\Im(d_p)\big)\big\}+\bar{\imath}\Big)\\
&+\upsilon^{d_p}(\upsilon^{h_J}-1)\mathbb{E}\big\{V\big(\Im(d_p)\big)\big\}\\
=&\upsilon^{d_p}\big(\upsilon^{h_J}-1-\upsilon^{h_J}\eta_1\big)\mathbb{E}\big\{V\big(\Im(d_p)\big)\big\}+\upsilon^{d_{p+1}}\bar{\imath}\\
=&\upsilon^{d_p}\natural(\upsilon)\mathbb{E}\big\{V\big(\Im(d_p)\big)\big\}+\upsilon^{d_{p+1}}\bar{\imath}
\end{aligned}\tag{30}
$$

with

$$
\natural(\upsilon)\triangleq\upsilon^{h_J}-1-\upsilon^{h_J}\eta_1.
$$

For any integer $a>0$, taking the summation on both sides of the above inequality from 0 to $a-1$ with respect to p, one obtains

$$
\begin{aligned}
&\upsilon^{d_a}\mathbb{E}\big\{V\big(\Im(d_a)\big)\big\}-\mathbb{E}\big\{V\big(\Im(d_0)\big)\big\}\\
\leqslant&\natural(\upsilon)\sum_{p=0}^{a-1}\upsilon^{d_p}\mathbb{E}\big\{V\big(\Im(d_p)\big)\big\}+\frac{\upsilon^{h_J}(1-\upsilon^{d_a})}{1-\upsilon^{h_J}}\bar{\imath}.
\end{aligned}\tag{31}
$$

Note that

$$
\natural(1)=-\eta_1<0,\quad \lim_{\upsilon\to\infty}\natural(\upsilon)=+\infty.
$$

Then, there exists a scalar $b>1$ such that $\natural(b)=0$, which indicates

$$
b^{d_a}\mathbb{E}\big\{V\big(\Im(d_a)\big)\big\}-\mathbb{E}\big\{V\big(\Im(d_0)\big)\big\}\leqslant\frac{b^{h_J}(1-b^{d_a})}{1-b^{h_J}}\bar{\imath}.\tag{32}
$$

Furthermore, it is derived from (32) that

$$
\mathbb{E}\big\{V\big(\Im(d_a)\big)\big\}\leqslant\frac{\mathbb{E}\big\{V\big(\Im(d_0)\big)\big\}}{b^{d_a}}+\frac{b^{h_J}(1-b^{d_a})}{b^{d_a}(1-b^{h_J})}\bar{\imath}.\tag{33}
$$

Combining (23) and (33), one has

$$
\begin{aligned}
&\mathbb{E}\big\{\|\Im(d_a)\|^2\big\}\\
\leqslant&\frac{\mathbb{E}\big\{V\big(\Im(d_a)\big)\big\}}{\lambda_{\min}(\Theta)}\\
\leqslant&\frac{\mathbb{E}\big\{V\big(\Im(d_0)\big)\big\}}{b^{d_a}\lambda_{\min}(\Theta)}+\frac{b^{h_J}(1-b^{d_a})}{b^{d_a}(1-b^{h_J})\lambda_{\min}(\Theta)}\bar{\imath}.
\end{aligned}\tag{34}
$$

By denoting

$$
\alpha_3(d_p)\triangleq\frac{b^{h_J}(1-b^{d_p})}{b^{d_p}(1-b^{h_J})\lambda_{\min}(\Theta)}\bar{\imath},
$$

one knows that

$$
\lim_{p\to\infty}\alpha_3(d_p)=\frac{\bar{\imath}}{\lambda_{\min}(\Theta)\eta_1}\triangleq\alpha_3.\tag{35}
$$

Furthermore, defining

$$
\alpha_1\triangleq\frac{1}{b},\quad \alpha_2\triangleq\frac{\mathbb{E}\big\{V\big(\Im(d_0)\big)\big\}}{\lambda_{\min}(\Theta)},
$$

it follows from (34)–(35) that

$$
\mathbb{E}\big\{\|\Im(d_p)\|^2\big\}\leqslant\alpha_1^{d_p}\alpha_2+\alpha_3.\tag{36}
$$

Based on Definition 1, the dynamics of the augmented system (19) is guaranteed to be EUBMS. Referring to formulas

(27), (29) and (35), it can be inferred that the AUB of $\|\Im(d_p)\|^2$ in mean-square sense is obtained as

$$\begin{aligned}\alpha_3 =&\frac{\bar{\iota}}{\lambda_{\min}(\Theta)\eta_1}\\ =&\frac{1}{\lambda_{\min}(\Theta)\eta_1}\left(\eta_2\sum_{i=1}^{n}\left(\frac{\theta^{[i]}\gamma^{[i]}}{\delta^{[i]}}\right)^2+\eta_3 h\bar{w}+\eta_4\bar{v}\right), \quad (37)\end{aligned}$$

and the proof is now complete. ∎

Remark 3: Theorem 1 offers a sufficient condition that ensures the augmented system (19) to be EUBMS. Note that the AUB presented in (22) is influenced by $\lambda_{\min}(\Theta)$, which poses a considerable challenge to the optimization of the PIO performance. To address this complexity, an additional constraint on the matrix Θ is proposed in the subsequent corollary.

Corollary 1: Under conditions in Theorem 1, if

$$\Theta \geqslant \mathbf{I}, \quad (38)$$

then the AUB of $\|\vartheta(k)\|^2$ in mean-square sense can be given by

$$\alpha_4 \triangleq \frac{1}{\eta_1}\left(\eta_2\sum_{i=1}^{n}\left(\frac{\theta^{[i]}\gamma^{[i]}}{\delta^{[i]}}\right)^2+\eta_3 h\bar{w}+\eta_4\bar{v}\right). \quad (39)$$

Proof: First, it is deduced from (38) that

$$\lambda_{\min}(\Theta) \geqslant 1. \quad (40)$$

Then, recalling the conditions in Theorem 1, the following relation is obtained:

$$\lim_{p\to\infty}\mathbb{E}\{\|\Im(d_p)\|^2\} \leqslant \frac{\bar{\iota}}{\lambda_{\min}(\Theta)\eta_1} \leqslant \frac{\bar{\iota}}{\eta_1} = \alpha_4, \quad (41)$$

which ends the proof. ∎

Remark 4: The AUB encapsulates the combined influences of external disturbances and the facilitation of communication through relaying on the estimation accuracy. As illustrated in (39), the AUB is intimately connected with several factors including the number of sensors, the sensor sampling intervals, the characteristics of the quantizers, and the maximal limits of external disturbances and channel noise. Furthermore, the AUB hinges on the parameters η_1, η_2, η_3, and η_4, which are derived from the resolution of the matrix inequality presented in (21). It is crucial to observe that, while (39) might not overtly incorporate the transmission power ϵ, this power plays a pivotal role in shaping estimation performance since it influences the solvability of the matrix inequality (21). In essence, the transmission power ϵ impacts the viability of satisfying the matrix inequality (21). The intricate dynamics between transmission power and estimation accuracy motivates an in-depth exploration in Section IV.

C. Design of the PIO

Building on the insights provided by Theorem 1 and Corollary 1, the focus now transitions towards the determination of observer gains, aimed at optimizing the dynamic performance of the PIO. We consider three cases where the PIO is designed, respectively, 1) for a minimized AUB, 2) for a fastest convergence rate of the error dynamics of the state estimation, and 3) for a desired trade-off between the estimation accuracy and the error convergence.

1) PIO-A: In this case, the gains of PIO-A, represented by $H_1^{[A]}$, $H_2^{[A]}$, and $H_3^{[A]}$, are meticulously computed to achieve the smallest possible AUB for the estimation error dynamics.

Theorem 2: Consider the augmented system (19) with the PIO (18). Let the positive scalar $\eta_1^{[A]}$ $(0 < \eta_1^{[A]} < 1)$ be given. Then, the augmented system (19) is EUBMS if there exist positive scalars $\eta_2^{[A]}$, $\eta_3^{[A]}$, $\eta_4^{[A]}$, positive definite matrices $\Theta_1^{[A]}$, $\Theta_2^{[A]}$, $\Theta_3^{[A]}$, and matrices $\mathcal{H}_1^{[A]}$, $\mathcal{H}_2^{[A]}$, $\mathcal{H}_3^{[A]}$ such that

$$\begin{cases}\Re^{(2)} = \begin{bmatrix}\Re^{(2)}_{(11)} & \star\\ \Re^{(2)}_{(21)} & \Re^{(2)}_{(22)}\end{bmatrix} < 0 & (42a)\\ \Theta^{[A]} \geqslant \mathbf{I} & (42b)\end{cases}$$

with

$$\begin{aligned}\Re^{(2)}_{(11)} \triangleq&\operatorname{diag}\{-\Theta^{[A]}+\eta_1^{[A]}\Theta^{[A]},\ -\eta_2^{[A]}\mathbf{I},\ -\eta_3^{[A]}\mathbf{I},\ -\eta_4^{[A]}\mathbf{I}\}\\ \Re^{(2)}_{(21)} \triangleq&\begin{bmatrix}\hat{\aleph}\mathcal{A}_2^{[A]} & \hat{\aleph}\mathcal{M}_2^{[A]} & \mathbf{0} & \mathbf{0}\\ \mathcal{A}_1^{[A]} & \mathcal{M}_1^{[A]} & \mathcal{B}_1^{[A]} & \mathcal{B}_2^{[A]}\end{bmatrix}\\ \Re^{(2)}_{(22)} \triangleq&-\mathbf{I}_2\otimes\Theta^{[A]}, \quad \mathcal{M}_1^{[A]} \triangleq \begin{bmatrix}-\bar{\iota}(\epsilon)\sqrt{\epsilon}\mathcal{H}_2^{[A]}\\ \bar{\iota}(\epsilon)\sqrt{\epsilon}\mathcal{H}_3^{[A]}\\ \mathbf{0}\end{bmatrix}\\ \mathcal{A}_1^{[A]} \triangleq&\begin{bmatrix}\Theta_1^{[A]}\bar{A}-\mathcal{H}_2^{[A]}\bar{C} & -\mathcal{H}_1^{[A]} & \mathcal{A}_{1,(13)}^{[A]}\\ \mathcal{H}_3^{[A]}\bar{C} & \Theta_2^{[A]} & \mathcal{A}_{1,(23)}^{[A]}\\ \mathbf{0} & \mathbf{0} & \Theta_3^{[A]}\bar{A}\end{bmatrix}\\ \mathcal{A}_2^{[A]} \triangleq&\begin{bmatrix}\mathbf{0} & \mathbf{0} & -\sqrt{\epsilon}\mathcal{H}_2^{[A]}\bar{C}\\ \mathbf{0} & \mathbf{0} & \sqrt{\epsilon}\mathcal{H}_3^{[A]}\bar{C}\\ \mathbf{0} & \mathbf{0} & \mathbf{0}\end{bmatrix}, \quad \mathcal{B}_1^{[A]} \triangleq \begin{bmatrix}\Theta_1^{[A]}\bar{B}\\ \mathbf{0}\\ \Theta_3^{[A]}\bar{B}\end{bmatrix}\\ \mathcal{M}_2^{[A]} \triangleq&\begin{bmatrix}-\sqrt{\epsilon}\mathcal{H}_2^{[A]}\\ \sqrt{\epsilon}\mathcal{H}_3^{[A]}\\ \mathbf{0}\end{bmatrix}, \quad \mathcal{B}_2^{[A]} \triangleq \begin{bmatrix}-\mathcal{H}_2^{[A]}G\\ \mathcal{H}_3^{[A]}G\\ \mathbf{0}\end{bmatrix}\\ \Theta^{[A]} \triangleq&\operatorname{diag}\{\Theta_1^{[A]},\ \Theta_2^{[A]},\ \Theta_3^{[A]}\}\\ \mathcal{A}_{1,(13)}^{[A]} \triangleq&-\mathcal{H}_2^{[A]}\bar{C}-\bar{\iota}(\epsilon)\sqrt{\epsilon}\mathcal{H}_2^{[A]}\bar{C}\\ \mathcal{A}_{1,(23)}^{[A]} \triangleq&\bar{\iota}(\epsilon)\sqrt{\epsilon}\mathcal{H}_3^{[A]}\bar{C}-\mathcal{H}_3^{[A]}\bar{C}.\end{aligned}$$

Furthermore, the gains of PIO-A are given by

$$\begin{aligned}H_1^{[A]} =&(\Theta_1^{[A]})^{-1}\mathcal{H}_1^{[A]}\\ H_2^{[A]} =&(\Theta_1^{[A]})^{-1}\mathcal{H}_2^{[A]}\\ H_3^{[A]} =&(\Theta_2^{[A]})^{-1}\mathcal{H}_3^{[A]}. \quad (43)\end{aligned}$$

Proof: Taking into account (21), (42a)–(42b) collectively, and introducing the notation $\eta_1^{[A]} \triangleq \eta_1$ and $\Theta^{[A]} \triangleq \Theta$ for the sake of consistency across notations, we establish the following relationship:

$$\Re^{(2)}_{(11)} = \Re^{(1)}_{(11)}. \quad (44)$$

Subsequently, by denoting

$$\begin{aligned}\mathcal{H}_1^{[A]} \triangleq&\Theta_1^{[A]}H_1^{[A]}\\ \mathcal{H}_2^{[A]} \triangleq&\Theta_1^{[A]}H_2^{[A]}\\ \mathcal{H}_3^{[A]} \triangleq&\Theta_2^{[A]}H_3^{[A]}, \quad (45)\end{aligned}$$

and pre-multiplying (21) with $\breve{\Theta}^{[A]} \triangleq \mathrm{diag}\{\mathbf{I}_4 \otimes \mathbf{I},\ \mathbf{I}_2 \otimes \Theta^{[A]}\}$ and post-multiplying (21) with $(\breve{\Theta}^{[A]})^T$, we can conclude that the inequality (42a) holds under the condition (21).

According to Theorem 1 and Corollary 1, (42a)–(42b) can guarantee that the augmented system (19) is EUBMS. Moreover, the definitions of $\mathcal{H}_1^{[A]}$, $\mathcal{H}_2^{[A]}$, $\mathcal{H}_3^{[A]}$ indicate that the gains of PIO-A can be designed as stated in (43). ■

It is shown in (39) that the expression of the AUB α_4 is related to $\eta_1^{[A]}$, $\eta_2^{[A]}$, $\eta_3^{[A]}$, $\eta_4^{[A]}$. Since $\eta_1^{[A]}$ is viewed as a known constant, the design of PIO-A can be formulated as the following optimization problem:

OP I:

$$\begin{aligned}\min_{\eta_2^{[A]},\eta_3^{[A]},\eta_4^{[A]}} \quad & \eta_2^{[A]}\sum_{i=1}^{n}\left(\frac{\theta^{[i]}\gamma^{[i]}}{\delta^{[i]}}\right)^2 + \eta_3^{[A]}h\bar{w} + \eta_4^{[A]}\bar{v} \\ \text{s.t.} \quad & \text{(42a) and (42b)} \\ & \eta_2^{[A]},\ \eta_3^{[A]},\ \eta_4^{[A]} > 0. \end{aligned} \tag{46}$$

The gains of PIO-A can be calculated by using Theorem 2 and then solving the convex optimization problem (46).

2) PIO-B: The gains of PIO-B, denoted as $H_1^{[B]}$, $H_2^{[B]}$, $H_3^{[B]}$, are determined to achieve the fastest convergence of the estimation error dynamics.

Theorem 3: Consider the augmented system (19) with the PIO (18). The augmented system (19) is EUBMS if there exist positive scalars $\eta_1^{[B]}$, $\eta_2^{[B]}$, $\eta_3^{[B]}$, $\eta_4^{[B]}$, positive definite matrices $\Theta_1^{[B]}$, $\Theta_2^{[B]}$, $\Theta_3^{[B]}$, Σ, and matrices $\mathcal{H}_1^{[B]}$, $\mathcal{H}_2^{[B]}$, $\mathcal{H}_3^{[B]}$ such that

$$\begin{cases} \Re^{(3)} = \begin{bmatrix} \Re^{(3)}_{(11)} & \star \\ \Re^{(3)}_{(21)} & \Re^{(3)}_{(22)} \end{bmatrix} < 0 & \text{(47a)} \\ \Re^{(4)} = \begin{bmatrix} \Re^{(4)}_{(11)} & \star \\ \Re^{(4)}_{(21)} & \Re^{(4)}_{(22)} \end{bmatrix} < 0 & \text{(47b)} \\ \Theta^{[B]} \geqslant \mathbf{I} & \text{(47c)} \end{cases}$$

with

$$\begin{aligned}
\Re^{(3)}_{(11)} &\triangleq -\Sigma, \quad \Re^{(3)}_{(21)} \triangleq \eta_1^{[B]}\mathbf{I}, \quad \Re^{(3)}_{(22)} \triangleq \Theta^{[B]} - 2\mathbf{I} \\
\Re^{(4)}_{(11)} &\triangleq \mathrm{diag}\{-\Theta^{[B]} + \Sigma,\ -\eta_2^{[B]}\mathbf{I},\ -\eta_3^{[B]}\mathbf{I},\ -\eta_4^{[B]}\mathbf{I}\} \\
\Re^{(4)}_{(21)} &\triangleq \begin{bmatrix} \hat{\aleph}\mathcal{A}_2^{[B]} & \hat{\aleph}\mathcal{M}_2^{[B]} & \mathbf{0} & \mathbf{0} \\ \mathcal{A}_1^{[B]} & \mathcal{M}_1^{[B]} & \mathcal{B}_1^{[B]} & \mathcal{B}_2^{[B]} \end{bmatrix} \\
\Re^{(4)}_{(22)} &\triangleq -\mathbf{I}_2 \otimes \Theta^{[B]}, \quad \mathcal{M}_1^{[B]} \triangleq \begin{bmatrix} -\bar{\iota}(\epsilon)\sqrt{\epsilon}\mathcal{H}_2^{[B]} \\ \bar{\iota}(\epsilon)\sqrt{\epsilon}\mathcal{H}_3^{[B]} \\ \mathbf{0} \end{bmatrix} \\
\mathcal{A}_1^{[B]} &\triangleq \begin{bmatrix} \Theta_1^{[B]}\bar{A} - \mathcal{H}_2^{[B]}\bar{C} & -\mathcal{H}_1^{[B]} & \mathcal{A}^{[B]}_{1,(13)} \\ \mathcal{H}_3^{[B]}\bar{C} & \Theta_2^{[B]} & \mathcal{A}^{[B]}_{1,(23)} \\ \mathbf{0} & \mathbf{0} & \Theta_3^{[B]}\bar{A} \end{bmatrix} \\
\mathcal{A}_2^{[B]} &\triangleq \begin{bmatrix} \mathbf{0} & \mathbf{0} & -\sqrt{\epsilon}\mathcal{H}_2^{[B]}\bar{C} \\ \mathbf{0} & \mathbf{0} & \sqrt{\epsilon}\mathcal{H}_3^{[B]}\bar{C} \\ \mathbf{0} & \mathbf{0} & \mathbf{0} \end{bmatrix}, \quad \mathcal{B}_1^{[B]} \triangleq \begin{bmatrix} \Theta_1^{[B]}\bar{B} \\ \mathbf{0} \\ \Theta_3^{[B]}\bar{B} \end{bmatrix} \\
\mathcal{M}_2^{[B]} &\triangleq \begin{bmatrix} -\sqrt{\epsilon}\mathcal{H}_2^{[B]} \\ \sqrt{\epsilon}\mathcal{H}_3^{[B]} \\ \mathbf{0} \end{bmatrix}, \quad \mathcal{B}_2^{[B]} \triangleq \begin{bmatrix} -\mathcal{H}_2^{[B]}G \\ \mathcal{H}_3^{[B]}G \\ \mathbf{0} \end{bmatrix} \\
\Theta^{[B]} &\triangleq \mathrm{diag}\{\Theta_1^{[B]},\ \Theta_2^{[B]},\ \Theta_3^{[B]}\} \\
\mathcal{A}^{[B]}_{1,(13)} &\triangleq -\mathcal{H}_2^{[B]}\bar{C} - \bar{\iota}(\epsilon)\sqrt{\epsilon}\mathcal{H}_2^{[B]}\bar{C} \\
\mathcal{A}^{[B]}_{1,(23)} &\triangleq \bar{\iota}(\epsilon)\sqrt{\epsilon}\mathcal{H}_3^{[B]}\bar{C} - \mathcal{H}_3^{[B]}\bar{C}.
\end{aligned}$$

Furthermore, the gains of PIO-B are given by

$$\begin{aligned} H_1^{[B]} &= (\Theta_1^{[B]})^{-1}\mathcal{H}_1^{[B]} \\ H_2^{[B]} &= (\Theta_1^{[B]})^{-1}\mathcal{H}_2^{[B]} \\ H_3^{[B]} &= (\Theta_2^{[B]})^{-1}\mathcal{H}_3^{[B]}. \end{aligned} \tag{48}$$

Proof: Based on the relation

$$(\Theta^{[B]} - \mathbf{I})(\Theta^{[B]})^{-1}(\Theta^{[B]} - \mathbf{I}) \geqslant 0, \tag{49}$$

we have

$$-(\Theta^{[B]})^{-1} \leqslant \Theta^{[B]} - 2\mathbf{I}. \tag{50}$$

From (47a), one has

$$\begin{bmatrix} -\Sigma & \star \\ \eta_1^{[B]}\mathbf{I} & -(\Theta^{[B]})^{-1} \end{bmatrix} < 0. \tag{51}$$

Applying the Schur Complement Lemma to the above inequality, we obtain

$$(\eta_1^{[B]})^2\Theta^{[B]} < \Sigma. \tag{52}$$

By denoting

$$\begin{aligned} \Theta^{[B]} &\triangleq \Theta, \quad \breve{\Theta}^{[B]} \triangleq \mathrm{diag}\{\mathbf{I}_4 \otimes \mathbf{I},\ \mathbf{I}_2 \otimes \Theta^{[B]}\} \\ \eta_1^{[B]} &\triangleq \sqrt{\eta_1}, \quad \mathcal{H}_1^{[B]} \triangleq \Theta_1^{[B]}H_1^{[B]} \\ \mathcal{H}_2^{[B]} &\triangleq \Theta_1^{[B]}H_2^{[B]}, \quad \mathcal{H}_3^{[B]} \triangleq \Theta_2^{[B]}H_3^{[B]}, \end{aligned}$$

and pre-multiplying the matrix in (21) with $\breve{\Theta}^{[B]}$ and post-multiplying it with $(\breve{\Theta}^{[B]})^T$, we can conclude that the condition (47b) holds. The proof is complete. ■

As stated in Theorem 1, the following relation is established:

$$\begin{aligned} &\mathbb{E}\{V(\Im(d_p))\} \\ &\leqslant \left(1 - (\eta_1^{[B]})^2\right)^{d_p}\mathbb{E}\{V(\Im(d_0))\} \\ &\quad + \frac{1}{(\eta_1^{[B]})^2}\left(\eta_2\sum_{i=1}^{n}\left(\frac{\theta^{[i]}\gamma^{[i]}}{\delta^{[i]}}\right)^2 + \eta_3 h\bar{w} + \eta_4\bar{v}\right). \end{aligned} \tag{53}$$

As elucidated in (53), the convergence rate of $\Im(d_p)$ is contingent upon the expression $1 - (\eta_1^{[B]})^2$. More specifically, a diminished value of $1 - (\eta_1^{[B]})^2$ leads to a more rapid convergence. Consequently, to ascertain the minimal value of $1 - (\eta_1^{[B]})^2$, and thereby secure the optimal convergence rate of $\Im(d_p)$, the strategy involves maximizing $\eta_1^{[B]}$. This maximization is pursued through the resolution of the subsequent optimization problems:

OP II:

$$\begin{aligned} \max \quad & \eta_1^{[B]} \\ \text{s.t.} \quad & \text{(47a) – (47c)} \\ & 0 < \eta_1^{[B]} < 1. \end{aligned} \tag{54}$$

Once optimization problem (54) is solved, the gains of PIO-B can be directly obtained by means of Theorem 3.

3) PIO-C: The gains of PIO-C, represented by $H_1^{[C]}$, $H_2^{[C]}$, and $H_3^{[C]}$, are formulated as linear combinations of the gains from PIO-A and PIO-B. This design approach enables PIO-C to simultaneously regulate the convergence rate and enhance the accuracy of estimation, offering a versatile solution to balance these critical aspects of system performance.

Theorem 4: Consider the augmented system (19) with the PIO (18). Let the positive scalar ν $(0<\nu<1)$ be given. Then, the augmented system (19) is EUBMS if the gain matrices $\mathcal{H}_1^{[C]}$, $\mathcal{H}_2^{[C]}$, $\mathcal{H}_3^{[C]}$ are determined by

$$\begin{aligned} H_1^{[C]} =&(\Theta_1^{[C]})^{-1}\mathcal{H}_1^{[C]} \\ H_2^{[C]} =&(\Theta_1^{[C]})^{-1}\mathcal{H}_2^{[C]} \\ H_3^{[C]} =&(\Theta_2^{[C]})^{-1}\mathcal{H}_3^{[C]} \end{aligned} \tag{55}$$

with

$$\begin{aligned} \Theta_1^{[C]} \triangleq&\nu\Theta_1^{[A]}+(1-\nu)\Theta_1^{[B]} \\ \Theta_2^{[C]} \triangleq&\nu\Theta_2^{[A]}+(1-\nu)\Theta_2^{[B]} \\ \mathcal{H}_1^{[C]} \triangleq&\nu\mathcal{H}_1^{[A]}+(1-\nu)\mathcal{H}_1^{[B]} \\ \mathcal{H}_2^{[C]} \triangleq&\nu\mathcal{H}_2^{[A]}+(1-\nu)\mathcal{H}_2^{[B]} \\ \mathcal{H}_3^{[C]} \triangleq&\nu\mathcal{H}_3^{[A]}+(1-\nu)\mathcal{H}_3^{[B]}. \end{aligned}$$

Proof: The proof of Theorem 4 is easily accessible from Theorems 2–3 and is therefore omitted here for space saving. ∎

Remark 5: Theorem 4 presents a strategy for configuring the PIO to achieve a balance between estimation precision and the rate at which errors converge. It is noteworthy that, within the framework prescribed by Theorem 4, the parameter ν offers flexibility and can be tailored to meet the unique performance demands of various real-world applications. This bespoke approach provides a significant benefit, enabling a focused enhancement of the PIO's dynamic characteristics, which in turn contributes to the improvement of the overall system state estimation performance.

Remark 6: This paper makes the following major contributions to the realm of PIO design for multi-rate systems, setting itself apart from existing literature through key innovations.

1) A novel component-based DaF relay protocol is introduced that facilitates the decoding of information from various encoders distributed across different locations. This enhancement significantly bolsters the reliability of information transmission over diverse communication distances and under varying resource constraints.
2) A PIO equipped with a tunable parameter is developed that allows for the simultaneous adjustment of the convergence rate and estimation accuracy. This dual-capability approach meets the nuanced performance needs encountered in real-world applications, providing a balanced solution that can be finely adjusted.
3) Comprehensive conditions are formulated that yield an explicit expression of the AUB for the estimation error dynamics. This crucial advancement enables a precise quantification of the cumulative impact arising from external disturbances and the supportive role of DaF relaying in communication, offering a clear metric for assessing system performance.

D. Design of Luenberger Observer

In fact, the Luenberger observer can be seen as a special case of PIO (18) by setting $H_1=0$. Next, we will focus on the design problem of the Luenberger observer. To do this, we first construct a Luenberger observer as follows:

$$\hat{x}(d_{p+1}) =\bar{A}\hat{x}(d_p)+H_4\big(\check{y}(d_p)-\hat{y}(d_p)\big) \tag{56}$$

where H_4 is the observer gain to be designed.

Defining the augmented state vector as

$$\wp(d_p)\triangleq \mathrm{col}\left\{\tilde{x}(d_p),\ \bar{x}(d_p)\right\},$$

the augmented system is presented by

$$\begin{aligned} \wp(d_{p+1}) =&\tilde{\mathcal{A}}_1\wp(d_p)+\aleph(d_p)\tilde{\mathcal{A}}_2\wp(d_p) \\ &+\tilde{\mathcal{M}}_1\xi(d_p)+\aleph(d_p)\tilde{\mathcal{M}}_2\xi(d_p) \\ &+\tilde{\mathcal{B}}_1\bar{w}(d_p)+\tilde{\mathcal{B}}_2 v(d_p) \end{aligned} \tag{57}$$

where

$$\begin{aligned} \tilde{\mathcal{A}}_1 &\triangleq \begin{bmatrix} \bar{A}-H_4\bar{C} & -H_4\bar{C}-\bar{\iota}(\epsilon)\sqrt{\epsilon}H_4\bar{C} \\ \mathbf{0} & \bar{A} \end{bmatrix} \\ \tilde{\mathcal{A}}_2 &\triangleq \begin{bmatrix} \mathbf{0} & -\sqrt{\epsilon}H_4\bar{C} \\ \mathbf{0} & \mathbf{0} \end{bmatrix},\quad \tilde{\mathcal{M}}_1\triangleq\begin{bmatrix} -\bar{\iota}(\epsilon)\sqrt{\epsilon}H_4 \\ \mathbf{0} \end{bmatrix} \\ \tilde{\mathcal{B}}_1 &\triangleq \begin{bmatrix} \bar{B} \\ \bar{B} \end{bmatrix},\quad \tilde{\mathcal{M}}_2\triangleq\begin{bmatrix} -\sqrt{\epsilon}H_4 \\ \mathbf{0} \end{bmatrix},\quad \tilde{\mathcal{B}}_2\triangleq\begin{bmatrix} -H_4G \\ \mathbf{0} \end{bmatrix}. \end{aligned}$$

With the Luenberger observer and the augmented system given above, we calculate the gains of the Luenberger observer from different perspectives to further enhance the estimation performance, which will be elaborated in the following corollaries.

1) Luenberger observer A: Luenberger observer A is designed to have a minimum AUB of the estimation error dynamics and the gain of this observer is denoted as $H_4^{[A]}$.

Corollary 2: Consider the augmented system (57) with the Luenberger observer (56). Let the positive scalar $\varsigma_1^{[A]}$ $(0<\varsigma_1^{[A]}<1)$ be given. Then, the augmented system (57) is EUBMS if there exist positive scalars $\varsigma_2^{[A]}$, $\varsigma_3^{[A]}$, $\varsigma_4^{[A]}$, positive definite matrices $\Phi_1^{[A]}$, $\Phi_2^{[A]}$, and matrix $\mathcal{H}_4^{[A]}$ such that

$$\begin{cases} \Lambda^{(1)}=\begin{bmatrix} \Lambda_{(11)}^{(1)} & \star \\ \Lambda_{(21)}^{(1)} & \Lambda_{(22)}^{(1)} \end{bmatrix}<0 & \text{(58a)} \\ \Phi^{[A]}\geqslant \mathbf{I} & \text{(58b)} \end{cases}$$

with

$$\begin{aligned} \Lambda_{(11)}^{(1)} \triangleq&\mathrm{diag}\{-\Phi^{[A]}+\varsigma_1^{[A]}\Phi^{[A]},\ -\varsigma_2^{[A]}\mathbf{I},\ -\varsigma_3^{[A]}\mathbf{I},\ -\varsigma_4^{[A]}\mathbf{I}\} \\ \Lambda_{(21)}^{(1)} \triangleq& \begin{bmatrix} \hat{\aleph}\tilde{\mathcal{A}}_2^{[A]} & \hat{\aleph}\tilde{\mathcal{M}}_2^{[A]} & \mathbf{0} & \mathbf{0} \\ \tilde{\mathcal{A}}_1^{[A]} & \tilde{\mathcal{M}}_1^{[A]} & \tilde{\mathcal{B}}_1^{[A]} & \tilde{\mathcal{B}}_2^{[A]} \end{bmatrix} \\ \Lambda_{(22)}^{(1)} \triangleq&-\mathbf{I}_2\otimes\Phi^{[A]},\quad \tilde{\mathcal{M}}_1^{[A]}\triangleq\begin{bmatrix} -\bar{\iota}(\epsilon)\sqrt{\epsilon}\mathcal{H}_4^{[A]} \\ \mathbf{0} \end{bmatrix} \\ \tilde{\mathcal{A}}_1^{[A]} \triangleq& \begin{bmatrix} \Phi_1^{[A]}\bar{A}-\mathcal{H}_4^{[A]}\bar{C} & -\mathcal{H}_4^{[A]}\bar{C}-\bar{\iota}(\epsilon)\sqrt{\epsilon}\mathcal{H}_4^{[A]}\bar{C} \\ \mathbf{0} & \Phi_2^{[A]}\bar{A} \end{bmatrix} \\ \tilde{\mathcal{A}}_2^{[A]} \triangleq& \begin{bmatrix} \mathbf{0} & -\sqrt{\epsilon}\mathcal{H}_4^{[A]}\bar{C} \\ \mathbf{0} & \mathbf{0} \end{bmatrix},\quad \tilde{\mathcal{M}}_2^{[A]}\triangleq\begin{bmatrix} -\sqrt{\epsilon}\mathcal{H}_4^{[A]} \\ \mathbf{0} \end{bmatrix} \end{aligned}$$

$$\tilde{\mathcal{B}}_1^{[A]} \triangleq \begin{bmatrix} \Phi_1^{[A]}\bar{B} \\ \Phi_2^{[A]}\bar{B} \end{bmatrix}, \quad \tilde{\mathcal{B}}_2^{[A]} \triangleq \begin{bmatrix} -\mathcal{H}_4^{[A]}G \\ \mathbf{0} \end{bmatrix}$$
$$\Phi^{[A]} \triangleq \text{diag}\{\Phi_1^{[A]},\ \Phi_2^{[A]}\}.$$

Furthermore, the optimization problem for the AUB of $\|\wp(d_p)\|^2$ is formulated as the following minimization task:

OP III:

$$\begin{aligned} \min_{\varsigma_2^{[A]},\varsigma_3^{[A]},\varsigma_4^{[A]}} \quad & \varsigma_2^{[A]} \sum_{i=1}^{n} \left(\frac{\theta^{[i]}\gamma^{[i]}}{\delta^{[i]}}\right)^2 + \varsigma_3^{[A]} h\bar{w} + \varsigma_4^{[A]}\bar{v} \\ \text{s.t.} \quad & \text{(58a) and (58b)} \\ & \varsigma_2^{[A]},\ \varsigma_3^{[A]},\ \varsigma_4^{[A]} > 0. \end{aligned} \tag{59}$$

Based on the solution to the optimization problem *OP III*, the gain of Luenberger observer A is given by

$$H_4^{[A]} = (\Phi_1^{[A]})^{-1}\mathcal{H}_4^{[A]}. \tag{60}$$

2) Luenberger observer B: Luenberger observer B is developed to attain the fastest convergence of the estimation error dynamics and the gain of this observer is denoted as $H_4^{[B]}$.

Corollary 3: Consider the augmented system (57) with the Luenberger observer (56). The augmented system (57) is EUBMS if there exist positive scalars $\varsigma_1^{[B]}$, $\varsigma_2^{[B]}$, $\varsigma_3^{[B]}$, $\varsigma_4^{[B]}$, positive definite matrices $\Phi_1^{[B]}$, $\Phi_2^{[B]}$, Ψ, and matrix $\mathcal{H}_4^{[B]}$ such that

$$\begin{cases} \Lambda^{(2)} = \begin{bmatrix} \Lambda_{(11)}^{(2)} & \star \\ \Lambda_{(21)}^{(2)} & \Lambda_{(22)}^{(2)} \end{bmatrix} < 0 & \text{(61a)} \\ \Lambda^{(3)} = \begin{bmatrix} \Lambda_{(11)}^{(3)} & \star \\ \Lambda_{(21)}^{(3)} & \Lambda_{(22)}^{(3)} \end{bmatrix} < 0 & \text{(61b)} \\ \Phi^{[B]} \geqslant \mathbf{I} & \text{(61c)} \end{cases}$$

with

$$\Lambda_{(11)}^{(3)} \triangleq -\Psi, \quad \Lambda_{(21)}^{(3)} \triangleq \varsigma_1^{[B]}\mathbf{I}, \quad \Lambda_{(22)}^{(3)} \triangleq \Phi^{[B]} - 2\mathbf{I}$$
$$\Lambda_{(11)}^{(4)} \triangleq \text{diag}\{-\Phi^{[B]} + \Psi,\ -\varsigma_2^{[B]}\mathbf{I},\ -\varsigma_3^{[B]}\mathbf{I},\ -\varsigma_4^{[B]}\mathbf{I}\}$$
$$\Lambda_{(21)}^{(4)} \triangleq \begin{bmatrix} \hat{\aleph}\tilde{\mathcal{A}}_2^{[B]} & \hat{\aleph}\tilde{\mathcal{M}}_2^{[B]} & \mathbf{0} & \mathbf{0} \\ \tilde{\mathcal{A}}_1^{[B]} & \tilde{\mathcal{M}}_1^{[B]} & \tilde{\mathcal{B}}_1^{[B]} & \tilde{\mathcal{B}}_2^{[B]} \end{bmatrix}$$
$$\Lambda_{(22)}^{(4)} \triangleq -\mathbf{I}_2 \otimes \Phi^{[B]}, \quad \tilde{\mathcal{M}}_1^{[B]} \triangleq \begin{bmatrix} -\bar{\iota}(\epsilon)\sqrt{\epsilon}\mathcal{H}_4^{[B]} \\ \mathbf{0} \end{bmatrix}$$
$$\tilde{\mathcal{A}}_1^{[B]} \triangleq \begin{bmatrix} \Phi_1^{[B]}\bar{A} - \mathcal{H}_2^{[B]}\bar{C} & -\mathcal{H}_4^{[B]}\bar{C} - \bar{\iota}(\epsilon)\sqrt{\epsilon}\mathcal{H}_4^{[B]}\bar{C} \\ \mathbf{0} & \Phi_2^{[B]}\bar{A} \end{bmatrix}$$
$$\tilde{\mathcal{A}}_2^{[B]} \triangleq \begin{bmatrix} \mathbf{0} & -\sqrt{\epsilon}\mathcal{H}_4^{[B]}\bar{C} \\ \mathbf{0} & \mathbf{0} \end{bmatrix}, \quad \tilde{\mathcal{M}}_2^{[B]} \triangleq \begin{bmatrix} -\bar{\iota}(\epsilon)\sqrt{\epsilon}\mathcal{H}_4^{[B]} \\ \mathbf{0} \end{bmatrix}$$
$$\tilde{\mathcal{B}}_1^{[B]} \triangleq \begin{bmatrix} \Phi_1^{[B]}\bar{B} \\ \Phi_2^{[B]}\bar{B} \end{bmatrix}, \quad \tilde{\mathcal{B}}_2^{[B]} \triangleq \begin{bmatrix} -\mathcal{H}_4^{[B]}G \\ \mathbf{0} \end{bmatrix}$$
$$\Phi^{[B]} \triangleq \text{diag}\{\Phi_1^{[B]},\ \Phi_2^{[B]}\}.$$

Furthermore, the optimization problem for the fastest convergence of the estimation error dynamics is formulated as the following maximization task:

OP IV:

$$\begin{aligned} \max \quad & \varsigma_1^{[B]} \\ \text{s.t.} \quad & \text{(61a)} - \text{(61c)} \\ & 0 < \varsigma_1^{[B]} < 1. \end{aligned} \tag{62}$$

In this case, the gain of Luenberger observer B is given by

$$H_4^{[B]} = (\Phi_1^{[B]})^{-1}\mathcal{H}_4^{[B]}. \tag{63}$$

3) Luenberger observer C: Luenberger Observer C, characterized by its gain $H_4^{[C]}$, is designed to offer a balanced trade-off between the convergence rate and the estimation deviation, aiming to optimize the overall performance by carefully adjusting these two critical aspects of the observer's functionality.

Corollary 4: Consider the augmented system (57) with the Luenberger observer (56). Let the positive scalar ν $(0 < \nu < 1)$ be given. Then, the augmented system (57) is EUBMS if the gain matrix $H_4^{[C]}$ is determined by

$$H_4^{[C]} = (\Phi_1^{[C]})^{-1}\mathcal{H}_4^{[C]} \tag{64}$$

with

$$\Phi_1^{[C]} \triangleq \nu\Phi_1^{[A]} + (1-\nu)\Phi_1^{[B]}$$
$$\mathcal{H}_4^{[C]} \triangleq \nu\mathcal{H}_4^{[A]} + (1-\nu)\mathcal{H}_4^{[B]}.$$

IV. Numerical simulation

In this section, we present a simulation example along with comparative results to validate the efficacy of the proposed PIO design scheme.

In the simulation, we consider a multi-rate system with the state update period $\jmath = 1$ which measured by $n = 3$ sensors. The system parameters are given as follows:

$$A = \begin{bmatrix} 0.9 & 0.01 \\ -0.5 & 0.11 \end{bmatrix}, \quad B = \begin{bmatrix} 1.1 \\ 1.2 \end{bmatrix}, \quad G = \begin{bmatrix} 1.1 \\ 1.2 \\ 1.3 \end{bmatrix}$$
$$C^{[1]} = \begin{bmatrix} 1.1 & 0.1 \end{bmatrix}, \quad C^{[2]} = \begin{bmatrix} 1.2 & 0.2 \end{bmatrix}$$
$$C^{[3]} = \begin{bmatrix} 1.3 & 0.3 \end{bmatrix}, \quad h = 2.$$

The external noise is set as $w(z_p) = 0.1\sin(z_p)$ with $\bar{w} = 0.1$ and the channel noise is given as $v(d_p) = 1.1\sin(1.1d_p)$ with $\bar{v} = 1.1$. The initial state is set as $x(z_0) = \begin{bmatrix} 2 & -2 \end{bmatrix}^T$, while the initial states of the PIO and the Luenberger observer are set to be zero. The parameters related to quantization and encoding are chosen as follows:

$$\theta^{[1]} = 10, \quad \theta^{[2]} = 20, \quad \theta^{[3]} = 30$$
$$\gamma^{[1]} = 2, \quad \gamma^{[2]} = 3, \quad \gamma^{[3]} = 4$$
$$\delta^{[1]} = 20, \quad \delta^{[2]} = 30, \quad \delta^{[3]} = 40.$$

In addition, the available transmission power is assumed to be $\epsilon = 1.6$ and the parameter μ is selected as 0.5.

A. Effectiveness and Advantages of Designed PIO

Based on the aforementioned parameter settings, the desired observer gains are derived by Theorem 4 and Corollary 4, under which simulation results are presented in Figs. 3–4. By using the PIO, the estimation error dynamics are plotted in Fig. 3, which verifies that the estimation errors are indeed

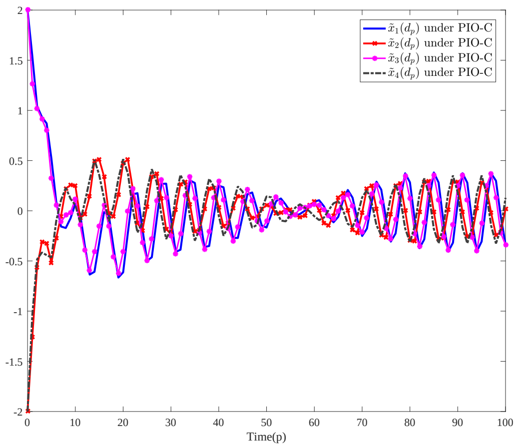

Fig. 3: Trajectories of $\tilde{x}(d_p)$ under PIO-C.

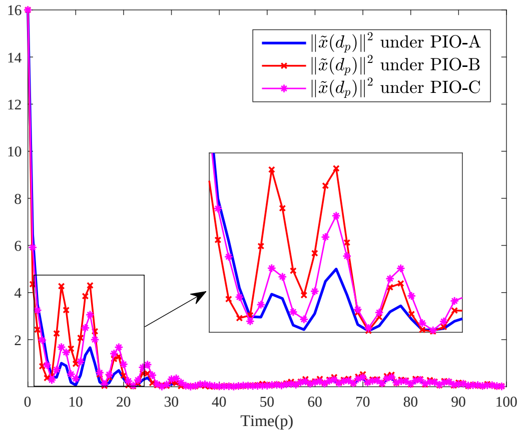

Fig. 5: Trajectories of $\|\tilde{x}(d_p)\|^2$ under different PIOs.

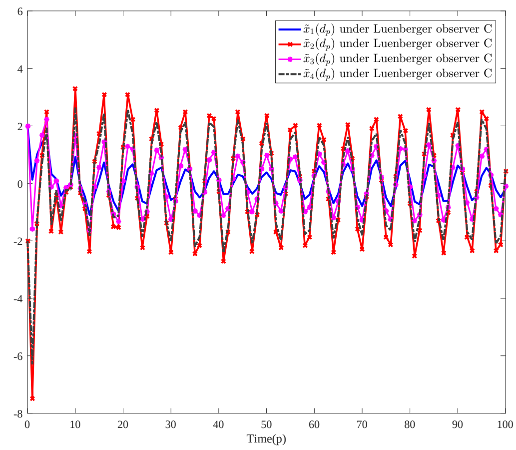

Fig. 4: Trajectories of $\tilde{x}(d_p)$ under Luenberger observer C.

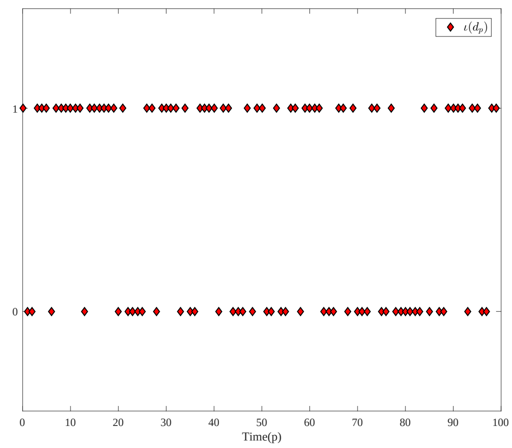

Fig. 6: The values of $\iota(d_p)$ with $\epsilon = 1.6$.

ultimately bounded. Fig. 4 depicts the estimation error dynamics under the Luenberger observer, which is regarded as a comparison to assess the superiority of the PIO. Evidently, the ultimately upper bound under the PIO is smaller than that under the Luenberger one, reflecting the better estimation performance of the designed PIO.

In Fig. 5, the trajectories of the estimation error dynamics under different PIOs are systematically compared. This analysis reveals several key observations: 1) the PIO-A, as formulated in Theorem 2, achieves a smaller AUB albeit with a slower convergence rate; 2) PIO-B, as delineated in Theorem 3, exhibits a more rapid convergence rate accompanied by a larger AUB; and 3) PIO-C, as proposed in Theorem 4, strikes a balance between estimation accuracy and error convergence rate. These findings underscore the nuanced trade-offs inherent in different PIO design strategies.

B. Effects of Available Transmission Power

The probability of packet dropout is closely tied to the transmission power, making the available transmission power, denoted as ϵ, a critical factor in determining estimation performance. In this simulation, with system parameters held constant, the relationship between varying transmission power ϵ and the upper bound of the estimation error is explored. Fig. 6 illustrates the incidence of packet dropout when $\epsilon = 1.6$. Furthermore, the minimum AUB of estimation error alongside the probabilities of packet dropouts for different values of transmission power ϵ are detailed in Table I. From this analysis, it is deduced that an escalation in the available transmission power ϵ is associated with a corresponding decline in both the probability of packet dropout and the AUB of estimation error, leading to the conclusion that higher available transmission power results in enhanced estimation accuracy.

TABLE I: The minimum AUB of estimation error and the probability of packet dropout with different transmission power ϵ

ϵ	1.1	1.6	2.1	2.6	3.1	3.6
$\iota(\epsilon)$	0.577	0.445	0.350	0.273	0.212	0.165
Minimum of α_4	0.401	0.364	0.346	0.313	0.293	0.264

V. CONCLUSIONS

In this paper, the PIO design challenge has been dealt with for multi-rate systems monitored by numerous sensors distributed across various locations. The underlying system allows for the sensor sampling intervals to deviate from the system update cycles, employing the lifting technique to navigate the complexities introduced by the multi-rate characteristics during the PIO analysis and design phases. A novel DaF relay strategy tailored for component-based systems has been introduced to address power-dependent packet dropouts in wireless transmissions. The impact of limited transmission power on the dropout rate has been thoroughly examined. An AUB for the mean-square estimation error has been established, which effectively encapsulates the cumulative influence of external disturbances and relay-assisted communication on estimation accuracy. Optimization problems have then been formulated within the observer gain design section with aim to balance estimation precision with convergence speed. The proposed estimation methodology's effectiveness has been corroborated through simulation, complemented by an in-depth examination of the interplay between estimation performance and restricted transmission power.

REFERENCES

[1] J. H. Ahrens, X. Tan and H. K. Khalil, Multirate sampled-data output feedback control with application to smart material actuated systems, *IEEE Transactions on Automatic Control*, vol. 54, no. 11, pp. 2518–2529, Nov. 2009.

[2] R. Caballero-Águila and J. Linares-Pérez, Distributed fusion filtering for uncertain systems with coupled noises, random delays and packet loss prediction compensation, *International Journal of Systems Science*, vol. 54, no. 2, pp. 371–390, Jan. 2023.

[3] J.-L. Chang, Applying discrete-time proportional integral observers for state and disturbance estimations, *IEEE Transactions on Automatic Control*, vol. 51, no. 5, pp. 814–818, May 2006.

[4] J. Cheng, L. Liang, H. Yan, J. Cao, S. Tang and K. Shi, Proportional-integral observer-based state estimation for Markov memristive neural networks with sensor saturations, *IEEE Transactions on Neural Networks and Learning Systems*, vol. 34, no. 12, pp. 9795–9805, Dec. 2023.

[5] D. Ciuonzo, A. Aubry and V. Carotenuto, Rician MIMO channel- and jamming-aware decision fusion, *IEEE Transactions on Signal Processing*, vol. 65, no. 15, pp. 3866–3880, Aug. 2017.

[6] R. Datta and Y. H. Joo, Fuzzy memory sampled-data controller design for PMSG-based WECS with stochastic packet dropouts, *IEEE Transactions on Fuzzy Systems*, vol. 31, no. 12, pp. 4421–4434, Dec. 2023.

[7] A. Elahi, A. Alf and H. Modares, H_∞ Consensus of homogeneous vehicular platooning systems with packet dropout and communication delay, *IEEE Transactions on Systems, Man, and Cybernetics: Systems*, vol. 52, no. 6, pp. 3680–3691, Jun. 2022.

[8] M. Elsheikh, R. Hille, A. Tatulea-Codrean and S. Kramer, A comparative review of multi-rate moving horizon estimation schemes for bioprocess applications, *Computers and Chemical Engineering*, vol. 146, art. no. 107219, Mar. 2021.

[9] Z. Feng, W. Xu and J. Cao, Distributed nash equilibrium computation under round-robin scheduling protocol, *IEEE Transactions on Automatic Control*, vol. 69, no. 1, pp. 339–346, Jan. 2024.

[10] X. Ge, Q.-L. Han, Q. Wu and X.-M. Zhang, Resilient and safe platooning control of connected automated vehicles against intermittent denial-of-service attacks, *IEEE/CAA Journal of Automatica Sinica*, vol. 10, no. 5, pp. 1234–1251, May 2023.

[11] H. Geng, Y. Liang, Y. Liu and F. E. Alsaadi, Bias estimation for asynchronous multi-rate multi-sensor fusion with unknown inputs, *Information Fusion*, vol. 39, pp. 139–153, Jan. 2018.

[12] F. Han, J. Liu, J. Li, J. Song, M. Wang and Y. Zhang, Consensus control for multi-rate multi-agent systems with fading measurements: The dynamic event-triggered case, *Systems Science & Control Engineering*, vol. 11, no. 1, art. no. 2158959, Dec. 2023.

[13] M. A. Hasabelnaby and A. Chaaban, Multi-pair computation for two-way intra cloud radio-access network communications, *IEEE Transactions on Wireless Communications*, vol. 21, no. 7, pp. 5586–5599, Jul. 2022.

[14] J. Hu, J. Li, G.-P. Liu, X. Yi and Z. Wu, Optimized distributed filtering for time-varying saturated stochastic systems with energy harvesting sensors over sensor networks, *IEEE Transactions on Signal and Information Processing Over Networks*, vol. 9, pp. 412–426, Jun. 2023.

[15] J. Hu, J. Li, H. Yan and H. Liu, Optimized distributed filtering for saturated systems with amplify-and-forward relays over sensor networks: A dynamic event-triggered approach, *IEEE Transactions on Neural Networks and Learning Systems*, in press, DOI: 10.1109/TNNLS.2023.3308192.

[16] C. Jia, J. Hu, X. Yi, H. Liu, J. Huang and Z. Cao, Recursive state estimation for a class of quantized coupled complex networks subject to missing measurements and amplify-and-forward relay, *Information Sciences*, vol. 630, pp. 53–73, Jun. 2023.

[17] D. Kumar, P. K. Singya, O. Krejcar and V. Bhatia, On performance of a SWIPT enabled FD CRN with HIs and imperfect SIC over α-θ fading channel, *IEEE Transactions on Cognitive Communications and Networking*, vol. 9, no. 1, pp. 99–113, Feb. 2023.

[18] M. Li, J. Liang and J. Qiu, Set-membership filtering for 2-D systems under uniform quantization and weighted try-once-discard protocol, *IEEE Transactions on Circuits and Systems II: Express Briefs*, vol. 70, no. 9, pp. 3474–3478, Sept. 2023.

[19] Y. Liang, T. Chen and Q. Pan, Multi-rate stochastic H_∞ filtering for networked multi-sensor fusion, *Automatica*, vol. 46, no. 2, pp. 437–444, Feb. 2010.

[20] Z.-Q. Liu, X. Ge, Q.-L. Han, Y.-L. Wang and X.-M. Zhang, Secure cooperative path following of autonomous surface vehicles under cyber and physical attacks, *IEEE Transactions on Intelligent Vehicles*, vol. 8, no. 6, pp. 3680–3691, Jun. 2023.

[21] L. Liu, Y.-J. Liu, S. Tong and Z. Gao, Relative threshold-based event-triggered control for nonlinear constrained systems with application to aircraft wing rock motion, *IEEE Transactions on Industrial Informatics*, vol. 18, no. 2, pp. 911–921, Feb. 2022.

[22] Y. Liu, Z. Wang, C. Liu, M. Coombes and W.-H. Chen, Auxiliary particle filtering over sensor networks under protocols of amplify-andforward and decode-and-forward relays, *IEEE Transactions on Signal and Information Processing over Networks*, vol. 8, pp. 883–893, Oct. 2022.

[23] T. Pan and Y. Yuan, A region-based relay pursuit scheme for a pursuit-evasion game with a single evader and multiple pursuers, *IEEE Transactions on Systems, Man, and Cybernetics: Systems*, vol. 53, no. 3, pp. 1958–1969, Mar. 2023.

[24] S. Roshany-Yamchi, M. Cychowski, R. R. Negenborn, B. De Schutter, K. Delaney and J. Connell, Kalman filter-based distributed predictive control of large-scale multi-rate systems: Application to power networks, *IEEE Transactions on Control Systems Technology*, vol. 21, no. 1, pp. 27–39, Jan. 2013.

[25] Y. Shao, L. Wang and Y. Xue, Distributed alamouti protocol for fullduplex decode-and-forward relaying networks, *IEEE Communications Letters*, vol. 26, no. 1, pp. 182–186, Jan. 2022.

[26] O. Shmuel, A. Cohen and O. Gurewitz, Compute-and-forward in large relaying systems: Limitations and asymptotically optimal scheduling, *IEEE Transactions on Information Theory*, vol. 67, no. 9, pp. 6243–6265, Sept. 2021.

[27] C. Li, Y. Liu, M. Gao and L. Sheng, Fault-tolerant formation consensus control for time-varying multi-agent systems with stochastic communication protocol, *International Journal of Network Dynamics and Intelligence*, vol. 3, no. 1, art. no. 100004, Mar. 2024.

[28] L. Sun, T. Wu and Y. Zhang, A defense strategy for false data injection attacks in multi-agent systems, *International Journal of Systems Science*, vol. 54, no. 16, pp. 3071–3084, 2023.

[29] S. M. J. A. Tabatabaee, M. Rajabzadeh and M. Towliat, A novel low-complexity GFDM relay communication system: Relay selection and filter-and-forward, *IEEE Transactions on Signal Processing*, vol. 69, pp. 5147–5158, Aug. 2021.

[30] H. Tan, B. Shen, Y. Liu, A. Alsaedi and B. Ahmad, Event-triggered multi-rate fusion estimation for uncertain system with stochastic nonlinearities and colored measurement noises, *Information Fusion*, vol. 36, pp. 313–320, Jul. 2017.

[31] W. Tang, E. Zhao, L. Sun and H. Gao, An active swing suppression control scheme of overhead cranes based on input shaping model predictive control, *Systems Science & Control Engineering*, vol. 11, no. 1, art. no. 2188401, 2023.

[32] V. S. Varma, S. Lasaulce, M. Debbah and S. E. Elayoubi, An energy-efficient framework for the analysis of mimo slow fading channels, *IEEE Transactions on Signal Processing*, vol. 61, no. 10, pp. 2647–2659, May 2013.

[33] V. S. Varma, A. M. de Oliveira, R. Postoyan, I. C.Morărescu and J. Daafouz, Energy-efficient time-triggered communication policies for wireless networked control systems, *IEEE Transactions on Automatic Control*, vol. 65, no. 10, pp. 4324–4331, Oct. 2019.

[34] R. Wang, B. Chen, Z. Hu, D. W. C. Ho and L. Yu. Distributed event-triggered fusion estimation for networked asynchronous multi-rate systems, *Information Fusion*, vol. 98, art. no. 101846, Oct. 2023.

[35] F. Wang, J. Liang, J. Lam, J. Yang and C. Zhao, Robust filtering for 2-D systems with uncertain-variance noises and weighted try-once-discard protocols, *IEEE Transactions on Systems, Man, and Cybernetics: Systems*, vol. 53, no. 5, pp. 2914–2924, May 2023.

[36] W. Wang and M. Wang, Adaptive neural event-triggered output-feedback optimal tracking control for discrete-time pure-feedback nonlinear systems, *International Journal of Network Dynamics and Intelligence*, vol. 3, no. 2, art. no. 100010, Jun. 2024.

[37] Y. Wang, H.-J. Liu and H.-L. Tan, An overview of filtering for sampled-data systems under communication constraints, *International Journal of Network Dynamics and Intelligence*, vol. 2, no. 3, art. no. 100011, Sep. 2023.

[38] Y. Wang, Z. Wang, L. Zou, Y. Chen and D. Yue, Distributed proportional-integral fuzzy state estimation over sensor networks under energy-constrained denial-of-service attacks, *IEEE Transactions on Cybernetics*, vol. 54, no. 1, pp. 641–654, Jan. 2024.

[39] A.-G. Wu and G. Duan, Design of PI observers for continuous-time descriptor linear systems, *IEEE Transactions on Systems, Man, and Cybernetics: Cybernetics*, vol. 36, no. 6, pp. 1423–1431, Dec. 2006.

[40] Y. Yan, H. Du, Q.-L. Han and W. Li, Discrete multi-objective switching topology sliding mode control of connected autonomous vehicles with packet loss, *IEEE Transactions on Intelligent Vehicles*, vol. 8, no. 4, pp. 2926–2938, Apr. 2023.

[41] C. Yang, J. Liang and W. Xu, PI observer-based synchronization control for singularly perturbed complex dynamical networks: An improved coding-decoding protocol scheme, *IEEE Transactions on Network Science and Engineering*, vol. 11, no. 1, pp. 858–871, Jan./Feb. 2024.

[42] L. Yang, Y. Xu, Z. Huang, H. Rao and D. E. Quevedo, Learning optimal stochastic sensor scheduling for remote estimation with channel capacity constraint, *IEEE Transactions on Industrial Informatics*, vol. 19, no. 3, pp. 2565–2573, Mar. 2023.

[43] M. Yao and G. Wei, Dynamic event-triggered control of continuous-time systems with random impulses, *IEEE/CAA Journal of Automatica Sinica*, vol. 10, no. 12, pp. 2292–2299, Dec. 2023.

[44] X. Yin, Z. Gao, D. Yue and S. Hu, Cloud-based event-triggered predictive control for heterogeneous NMASs under both DoS attacks and transmission delays, *IEEE Transactions on Systems, Man, and Cybernetics: Systems*, vol. 52, no. 12, pp. 7482–7493, Dec. 2022.

[45] T. Youssef, M. Chadli, H. R. Karimi and M. Zelmat, Design of unknown inputs proportional integral observers for T-S fuzzy models, *Neurocomputing*, vol. 123, pp. 156–165, Jan. 2014.

[46] Y. Zhang, L. Zou, Y. Liu, D. Ding and J. Hu, A brief survey on nonlinear control using adaptive dynamic programming under engineering-oriented complexities, *International Journal of Systems Science*, vol. 54, no. 8, pp. 1855–1872, 2023.

[47] Y. Zhang, Z. Peng, G. Wen, J. Wang and T. Huang, Optimal stealthy linear man-in-the-middle attacks with resource constraints on remote state estimation, *IEEE Transactions on Systems, Man, and Cybernetics: Systems*, vol. 54, no. 1, pp. 445–456, Jan. 2024.

[48] D. Zhao, Z. Wang, G. Wei and W. Sheng, Partial-neurons-based proportional-integral observer design for artificial neural networks: A multiple description encoding scheme, *IEEE Transactions on Neural Networks and Learning Systems*, vol. 35, no. 5, pp. 6393–6407, May 2024.

Di Zhao received the B.Sc. degree in Mathematics from Jilin Normal University, Siping, China, in 2013 and the Ph.D. degree in Control Science and Engineering from University of Shanghai for Science and Technology, Shanghai, China, in 2020. She is currently an Associate Research Professor with the Business School, University of Shanghai for Science and Technology, Shanghai, China.

From August 2020 to April 2024, she was a Postdoctoral Research Fellow with the College of Science, University of Shanghai for Science and Technology, Shanghai, China. From November 2018 to November 2019, she was a visiting Ph.D. student in the Department of Computer Science, Brunel University London, Uxbridge, U.K.. From March to June 2018, she was a Research Associate in the Department of Mathematics, City University of Hong Kong, Hong Kong.

Dr. Zhao's research interests include PID control, proportional-integral observer, networked control systems and cyber-physical systems. She is currently a reviewer for some international journals.

Zidong Wang (Fellow, IEEE) received the B.Sc. degree in mathematics from Suzhou University, Suzhou, China, in 1986, and the M.Sc. degree in applied mathematics and the Ph.D. degree in electrical engineering from Nanjing University of Science and Technology, Nanjing, China, in 1990 and 1994, respectively.

From 1990 to 2002, he held teaching and research appointments in universities in China, Germany, and the U.K. He is currently a Professor of Dynamical Systems and Computing with the Department of Computer Science, Brunel University London, Uxbridge, U.K. He has authored number of papers in international journals. His research interests include dynamical systems, signal processing, bioinformatics, and control theory and applications.

Prof. Wang is a member of the Academia Europaea and the European Academy of Sciences and Arts, an Academician of the International Academy for Systems and Cybernetic Sciences, a fellow of the Royal Statistical Society, and a member of program committee for many international conferences. He holds of the Alexander von Humboldt Research Fellowship of Germany, the JSPS Research Fellowship of Japan, William Mong Visiting Research Fellowship of Hong Kong. He serves (or has served) as the Editor-in-Chief for *International Journal of Systems Science*, *Neurocomputing*, *Systems Science & Control Engineering*, and an Associate Editor for 12 international journals including *IEEE Transactions on Automatic Control*, *IEEE Transactions on Control Systems Technology*, *IEEE Transactions on Neural Networks*, *IEEE Transactions on Signal Processing, and IEEE Transactions on Systems, Man, and Cybernetics–Part C: Applications and Reviews*.

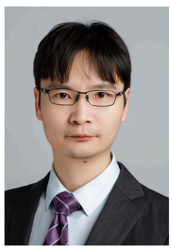

Derui Ding (Senior Member, IEEE) received both the B.Sc. degree in Industry Engineering in 2004 and the M.Sc. degree in Detection Technology and Automation Equipment in 2007 from Anhui Polytechnic University, Wuhu, China, and the Ph.D. degree in Control Theory and Control Engineering in 2014 from Donghua University, Shanghai, China. He is currently a Senior Research Fellow with the School of Science, Computing and Engineering Technologies, Swinburne University of Technology, Melbourne, VIC, Australia. His research interests include nonlinear stochastic control and filtering, as well as distributed control, filtering and optimization.

He was the recipient of the 2021 Nobert Wiener Review Award from IEEE/CAA Journal of Automatica Sinica, and the 2020 and 2022 Andrew P. Sage Best Transactions Paper Awards from the IEEE Systems, Man, and Cybernetics (SMC) Society. He is a *Senior Member* of the Chinese Association of Automation (CAA). He is serving as an Associate Editor for *IEEE Transactions on Industrial Informatics*, *IEEE/CAA Journal of Automatica Sinica*, *Neurocomputing* and *IET Control Theory* & *Applications*.

Qing-Long Han (Fellow, IEEE) received the B.Sc. degree in Mathematics from Shandong Normal University, Jinan, China, in 1983, and the M.Sc. and Ph.D. degrees in Control Engineering from East China University of Science and Technology, Shanghai, China, in 1992 and 1997, respectively.

Professor Han is Pro Vice-Chancellor (Research Quality) and a Distinguished Professor at Swinburne University of Technology, Melbourne, Australia. He held various academic and management positions at Griffith University and Central Queensland University, Australia. His research interests include networked control systems, multi-agent systems, time-delay systems, smart grids, unmanned surface vehicles, and neural networks.

Professor Han was awarded the 2024 IEEE Dr.-Ing. Eugene Mittelmann Achievement Award (the Highest Award in industrial electronics), the 2021 Norbert Wiener Award (the Highest Award in systems science and engineering, and cybernetics) and the 2021 M. A. Sargent Medal (the Highest Award of the Electrical College Board of Engineers Australia). He was the recipient of the IEEE Systems, Man, and Cybernetics Society Andrew P. Sage Best Transactions Paper Award in 2019, 2020, and 2022, respectively, the IEEE/CAA Journal of Automatica Sinica Norbert Wiener Review Award in 2020, and the IEEE Transactions on Industrial Informatics Outstanding Paper Award in 2020.

Professor Han is a Member of the Academia Europaea (The Academy of Europe). He is a Fellow of The International Federation of Automatic Control (FIFAC), an Honorary Fellow of The Institution of Engineers Australia (HonFIEAust), and a Fellow of Chinese Association of Automation (FCAA). He is a Highly Cited Researcher in both Engineering and Computer Science (Clarivate). He has served as an AdCom Member of IEEE Industrial Electronics Society (IES), a Member of IEEE IES Fellows Committee, a Member of IEEE IES Publications Committee, Chair of IEEE IES Technical Committee on Network-Based Control Systems and Applications, and the Co-Editor-in-Chief of IEEE Transactions on Industrial Informatics. He is currently the President-Elect, an Executive Board Member, and a Steering Committee Member of Asian Control Association (ACA). He is currently the Editor-in-Chief of IEEE/CAA Journal of Automatica Sinica and the Co-Editor of Australian Journal of Electrical and Electronic Engineering.

Guoliang Wei received the B.Sc. degree in mathematics from Henan Normal University, Xinxiang, China, in 1997 and the M.Sc. degree in applied mathematics and the Ph.D. degree in control engineering, both from Donghua University, Shanghai, China, in 2005 and 2008, respectively. He is currently a Professor with the Business School, University of Shanghai for Science and Technology, Shanghai, China.

From March 2010 to May 2011, he was an Alexander von Humboldt Research Fellow in the Institute for Automatic Control and Complex Systems, University of Duisburg-Essen, Germany. From March 2009 to February 2010, he was a postdoctoral research fellow in the Department of Information Systems and Computing, Brunel University, Uxbridge, U.K., sponsored by the Leverhulme Trust of the U.K. From June to August 2007, he was a Research Assistant at the University of Hong Kong. From March to May 2008, he was a Research Assistant at the City University of Hong Kong.

His research interests include nonlinear systems, stochastic systems, and bioinformatics. He has published more than 100 papers in refereed international journals. He is a very active reviewer for many international journals.